Physics and Chemistry of the Earth 127 (2022) 103157

Contents lists available at ScienceDirect

Physics and Chemistry of the Earth

journal homepage: www.elsevier.com/locate/pce

Probabilistic Seismic Hazard Analysis (PSHA) to estimate the input ground motions for Co-seismic landslide hazard assessment: A case study on Himalayan highways, Sikkim India

Saurav Kumar [a,*], Aniruddha Sengupta [a], Reginald Hermanns [b], John Dehls [b], Rajinder Kr Bhasin [c], Ivanna Penna [b], Vikram Gupta [d]

[a] Dept. of Civil Engg, IIT Kharagpur, 72130, India
[b] Geological Survey of Norway, Trondheim, Norway
[c] Norwegian Geotechnical Institute, Oslo, Norway
[d] Wadia Institute of Himalayan Geology, Dehardun, India

ARTICLE INFO

Keywords:
Seismic hazard
PSHA
Sikkim
PGA
Ground motion

ABSTRACT

Sikkim, the North-Eastern state of India, along with its neighbouring region is recognized as a part of the 'Alpine-Himalayan global seismic belt', which is one of the most seismically active areas of the world. Four significant earthquakes with a magnitude higher than Mw = 8.0 were reported in this area in earlier years of 1897, 1905, 1934, and 1950. The 2011 (M_w = 6.9) Sikkim and 2015 (M_w = 7.8) Gorkha Nepal earthquakes call attention to the need for a more accurate understanding of seismic characteristics in the Sikkim and their nearby region to minimize loss of life and properties due to future earthquakes and related co-seismic hazards. This study aims to estimate the Peak Ground Acceleration (PGA) having a known Probability of Exceedance (PoE) along Gangtok to Lachung and Gangtok to Tsomgo Lake; two strategic highways within Sikkim. The PGA with a known PoE is an essential input required for earthquake-triggered landslide susceptibility analysis on a regional scale as well as for the dynamic slope stability assessment of the prevailing hill slopes along the highways corridor in Sikkim. Therefore, a Probabilistic Seismic Hazard Analysis (PSHA) of the highway corridors in Sikkim is presented utilizing the updated earthquake catalogue, modified seismic sources, and next-generation attenuation relationships. The Uniform Hazard Spectra (UHS) and total hazard curves corresponding to the bedrock site conditions are generated employing 'EZ-FRISK' software. The variations of PGA having a 10% PoE in 50-years along the highways are estimated to identify the critical sections based on the ground acceleration parameter.

1. Introduction

Earthquakes in hilly regions can trigger extensive landslides (Keefer 1984; Xu et al., 2014). These co-seismic landslides are liable for significant societal impacts, such as loss of life, damage to public buildings, residential buildings, and several lifeline structures (road corridors, railway tracks, etc). They also hinder post-earthquake emergency relief efforts (Godt et al., 2008). These earthquake-triggered landslides are abundant in the Himalayan region, which is known for their high seismicity, intense rainfall, steep slopes, and large relative relief. The Himalayas and their nearby areas have witnessed many catastrophic co-seismic landslides in the past. The 2015 Nepal Earthquake (M_w = 7.8) initiated more than 20000 landslides (Roback et al., 2018). The 2011 Sikkim Earthquake of M_w 6.9 triggered 1196 landslides (Martha et al., 2015). Ghosh et al. (2012) have recorded 196 new and 14 reactivated landslides on the Darjeeling-Sikkim Himalayan roads in their post-earthquake field studies.

The PGA with a known PoE is a crucial parameter for earthquake-triggered landslide susceptibility analysis on a regional scale (Jibson 2007; Saygili and Rathje 2008) as well as site-specific dynamic analysis of slope (Jibson 2011). Generally, two methods, PSHA and Deterministic Seismic Hazard Analysis (DSHA) are adopted for the quantification of PGA, which is likely to be experienced at a specific site as a result of the occurrence of the seismic event in future. The DSHA method considers

* Corresponding author.
E-mail addresses: sauravmishra.kumar@gmail.com (S. Kumar), sengupta@civil.iitkgp.ac.in (A. Sengupta), reginald.hermanns@ngu.no (R. Hermanns), john.dehls@ngu.no (J. Dehls), rajinder.kumar.bhasin@ngi.no (R.K. Bhasin), Ivanna.Penna@ngu.no (I. Penna), vgupta@wihg.res.in (V. Gupta).

https://doi.org/10.1016/j.pce.2022.103157
Received 22 April 2021; Received in revised form 2 December 2021; Accepted 14 May 2022
Available online 19 May 2022
1474-7065/

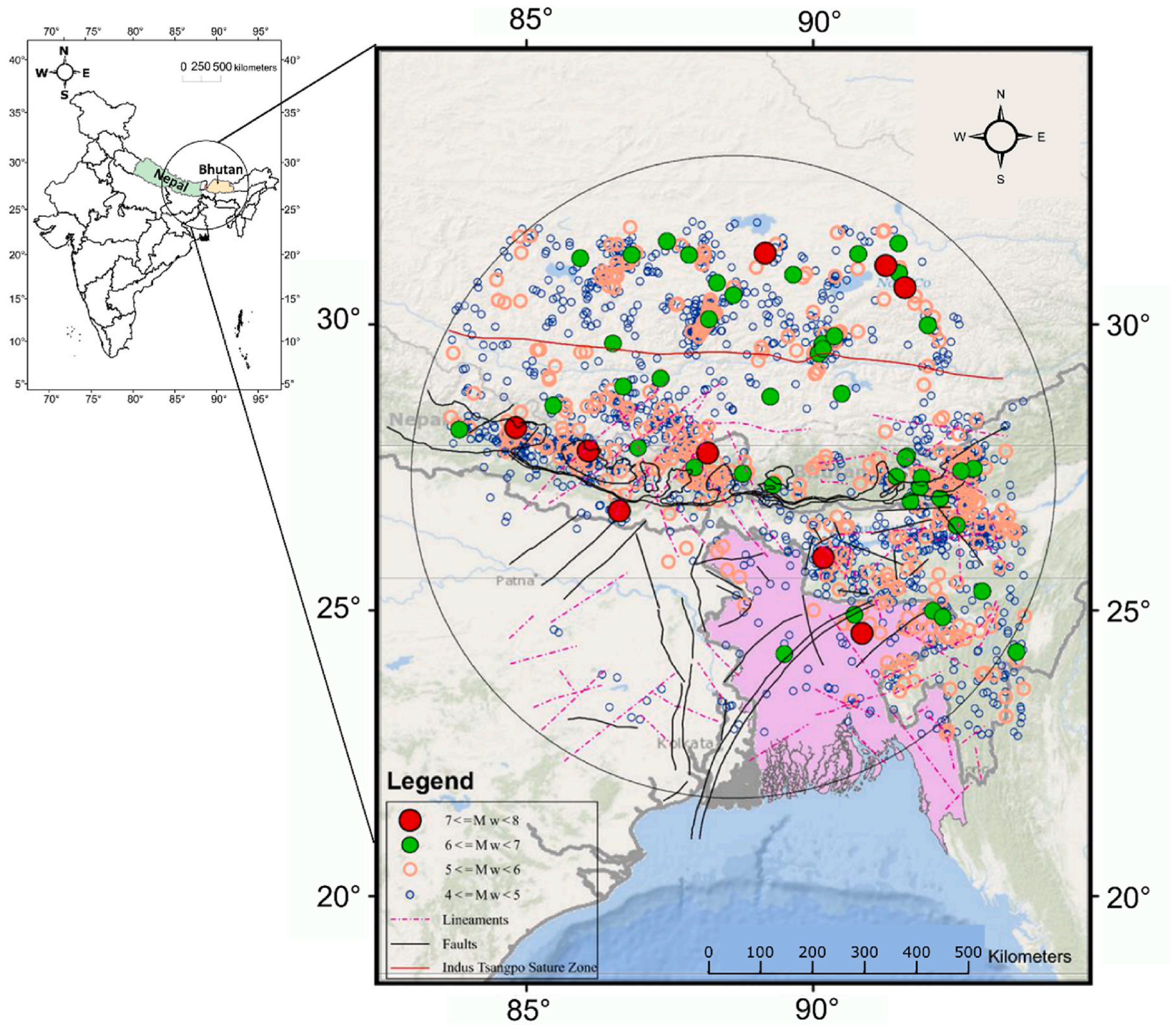

Fig. 1. Tectonic features of the study area with earthquake distribution.

only the occurrence of a specific earthquake scenario (worst scenario earthquake) at a fixed source for the estimation of PGA at the site under investigation (Kramer 1996; Bommer 2002; Baker 2008). This method ignores the effect of all triggered earthquakes other than the worst scenario earthquake (Reiter 1990; Krinitzsky 2002). Whereas, the PSHA incorporates the likelihood of all the seismic events from various possible seismic sources which can cause damages. It provides a framework in which spatial and temporal uncertainties associated with seismic events, can be recognized, quantified and integrated to deliver a more comprehensive portrayal of the seismic hazard (Kramer 1996). Further, it deals reasonably with various uncertainties that include the size, location, and resulting ground motions of future earthquakes employing the total probability theorem (Cornell 1968; McGuire, 1977; Kramer 1996; Baker 2008). Further, it has gained considerable importance in risk and safety analysis. Recently, numerous researchers have been developing region-specific seismic hazard parameters, across the globe by using the conventional PSHA approach (Zhang et al., 1999; Mezcua et al., 2011; Khan et al., 2013; Sil et al., 2013; Kavand and Alielahi, 2017; Waseem et al., 2019; Abdulnaby et al., 2020). The seismic behaviour of India has been extensively studied by researchers. These studies have been executed for the whole country at a macro level as well as for particular regions of the country, states, and cities of interest. In India, the initial studies are subjective and deterministic based on historical earthquake records, geology, and tectonics (Tandon 1956; Krishna 1959; Guha 1962). The first comprehensive PGA hazard map using the probabilistic approach was presented by Khattri et al. (1984) for entire India having a Return Period (RP) of 476-years Bhatia et al. (1999) presented the PGA hazard map of 10% PoE in 50-years for India and the neighbouring areas. Parvez et al. (2003) used a deterministic approach to prepare a seismic hazard map of India and the nearby regions. Further, the results obtained in this study are compared with the results of the probabilistic approach given by Khattri et al. (1984) and Bhatia et al. (1999). The National Disaster Management Authority (NDMA) (2010), and Nath and Thingbaijam (2012) reported the probabilistic seismic hazard map for the entire country. Nath and Thingbaijam (2012), in their study, used various Ground Motion Prediction Equations (GMPEs) corresponding to various seismotectonic regions of the country. Whereas, NDMA (2010) has presented the PGA map of the country considering the GMPE developed from the simulated ground motions. The seismic hazard studies of the earthquake-prone north--eastern region of India have been performed by several researchers (Parvez and Ram 1997; Malik et al., 2006; Das et al., 2016). Some of the major Indian cities where studies have been performed include Mumbai (Kanth and Iyengar 2006), Delhi (Iyengar and Ghosh 2004), Kolkata (Mohanty and Walling 2008), and Patna (Anbazhagan et al., 2019). The detailed seismic hazard analysis has been done for quantification of ground motion at important sites like the archaeological site at Kancheepuram in Tamilnadu, for important ports and Karkapur atomic power station of the Indian state of Gujrat (Corigliano et al., 2012; Shukla and Choudhury 2012; Mohanty and Verma 2013).

The PSHA comprises of various steps, including the identification and delineation of potential seismic sources, determination of seismic

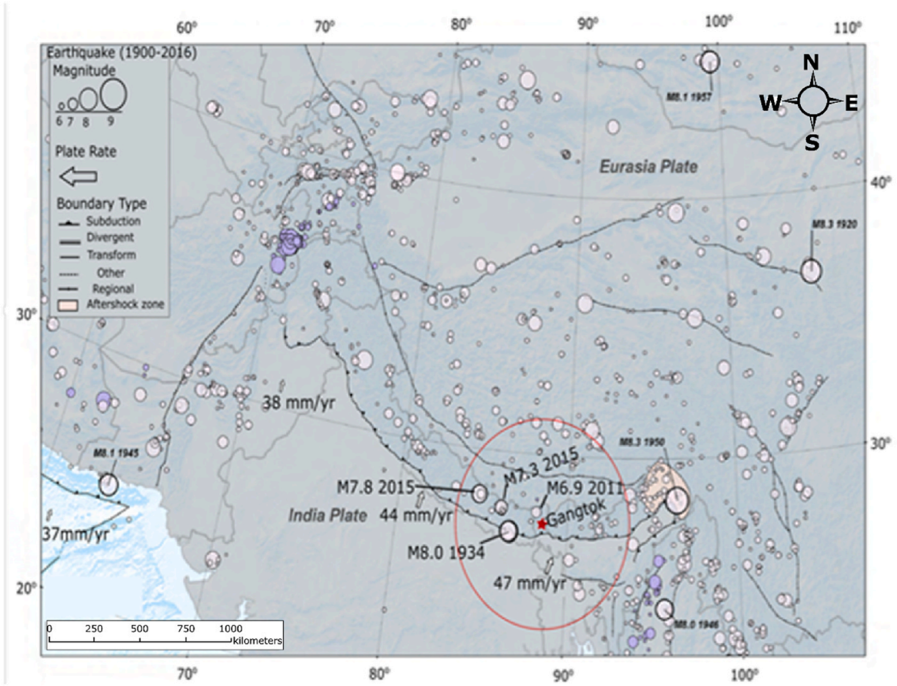

Fig. 2. Tectonic setting of the Himalayas with earthquake distribution and plate movement. (Source: USGS)

parameters of considered seismic sources, selection of suitable attenuation models, and estimation of ground motion parameters at bedrock with a known PoE. All the above-mentioned steps are explained in the subsequent parts. All the calculations related to the hazard analysis are done using a software package, "EZ-FRISK'' (Version 7.65, Risk Engineering) (Fugro Consultants Inc, 2014). All the obtained ground acceleration results correspond to the bedrock site condition. The hazard calculation has been done for a grid spaced at 0.05°, covering a rectangular area that contains the North Sikkim Highway. The UHS has been computed corresponding to a RP of 474.6-years at four important sites (Gangtok, Yumthang, Mangan, and Tsomgo Lake) located on the North Sikkim Highway. Further, a comparative assessment of results obtained from the present study and previous hazard studies for Gangtok, the capital city of Sikkim is presented.

2. Tectonics features and geology of the study area

The high seismic activities in the Himalayas are predominantly because of the collision between the Indian and the Eurasian plates (Figs. 1 and 2). The relative rate of convergence between these two plates is 40–50 mm/yr (Kayal 2001; Kumar et al., 2007). A large amount of strain accumulated by this collision is the prime cause of the intense seismicity, which in turn resulted in a tectonically active Himalayan belt. Four significant earthquakes of magnitude greater than Mw = 8.0 were reported in this area in earlier years of 1897, 1905, 1934, and 1950. Sikkim, the North-Eastern state of India is situated in the eastern part of the Himalayas (Fig. 3) and shares its boundary with Bhutan, Nepal, and Tibet on the East, West, and North, respectively. Sikkim and its neighbouring regions are recognized as a part of the "Alpine-Himalayan seismic belt". The seismicity in this area is generally linked with the tectonic activity along with the well-known tectonic structures, Main Boundary Thrust (MBT) and Main Central Thrust (MCT). In addition to MBT and MCT, other important tectonic structures in this region are SW–NE trending Kanchanjangha lineament, the WNW–ESE trending Golpara lineament, and two near-parallel SSE-NNW trending Gangtok and Tista lineaments (Figs. 3 and 4).

Tectonically, the Sikkim Himalayan region can be divided into a) Sub Himalayan Domain (SHD), b) Inner or Lesser Himalayan Domain (LHD), c) Higher Himalayan Domain (HHD) and d) Tethyan Sedimentary Sequence (TSS) Zone (Fig. 4). All these different geo-tectonic zones are separated from each other by reverse faults. The MBT separates SHD from LHD whereas the MCT demarcates the boundary of HHD and LHD. The exact location of MCT is controversial in Sikkim (Sinha-Roy, 1982). A zone of high deformation associated with MCT is termed as Main Central Thrust Zone (MCTZ). The SHD comprises deposits of the Siwaliks of mollase types. The LHD comprises carbonate rocks, a thin strip of Gondwana rocks, and a thick meta-sedimentary sequence belonging to the Gorubathan Formation of the Daling group. The HHD consists of medium to a high-grade crystalline rock known as Higher Himalayan Crystalline (HHC). HHC is dominant in pelitic schist with intermittent quartzites and calcium-silicate rocks. The Tethyan zone which merges into the Tibetan plateau comprises a thick pile of fossiliferous Ordovician to Carboniferous sediments (Gansser 1964; Acharyya 1989, 1992).

3. Compilation and processing of earthquake catalogue

The preparation of an earthquake catalogue is a necessary step for performing seismic hazard analysis of an area. It helps in the delineation of the seismic sources and characterization of its important seismic parameters, such as rate of seismicity (λ), the maximum magnitude of the earthquake (M_{max}), and Gutenberg–Richter seismic parameters (a and b). For this study, earthquake data has been compiled from various sources namely the United States Geological Survey (USGS), International Seismological Centre (ISC), Geological Survey of India (GSI), and Indian Meteorological Department (IMD) over a period of 1900–2018 within an area of 500 km radius from Gangtok, the capital city of Sikkim. We have also considered the regional earthquake data of Kolathayar et al. (2012) and Nath et al. (2017). Further, the compiled earthquakes from different sources are manually checked and the duplicate events based on their magnitude, time of occurrence, and locations are removed. we have preferred the ISC catalogue followed by the USGS catalogue and regional catalogue. The earthquake events reported in moment magnitude (Mw) has been preferred first. When more than one Mw magnitudes are reported for the same earthquake, in such cases the Mw magnitude reported by the Global Centroid Moment Tensor (GCMT) catalogue has been selected. The final catalogue of 1220 events consists

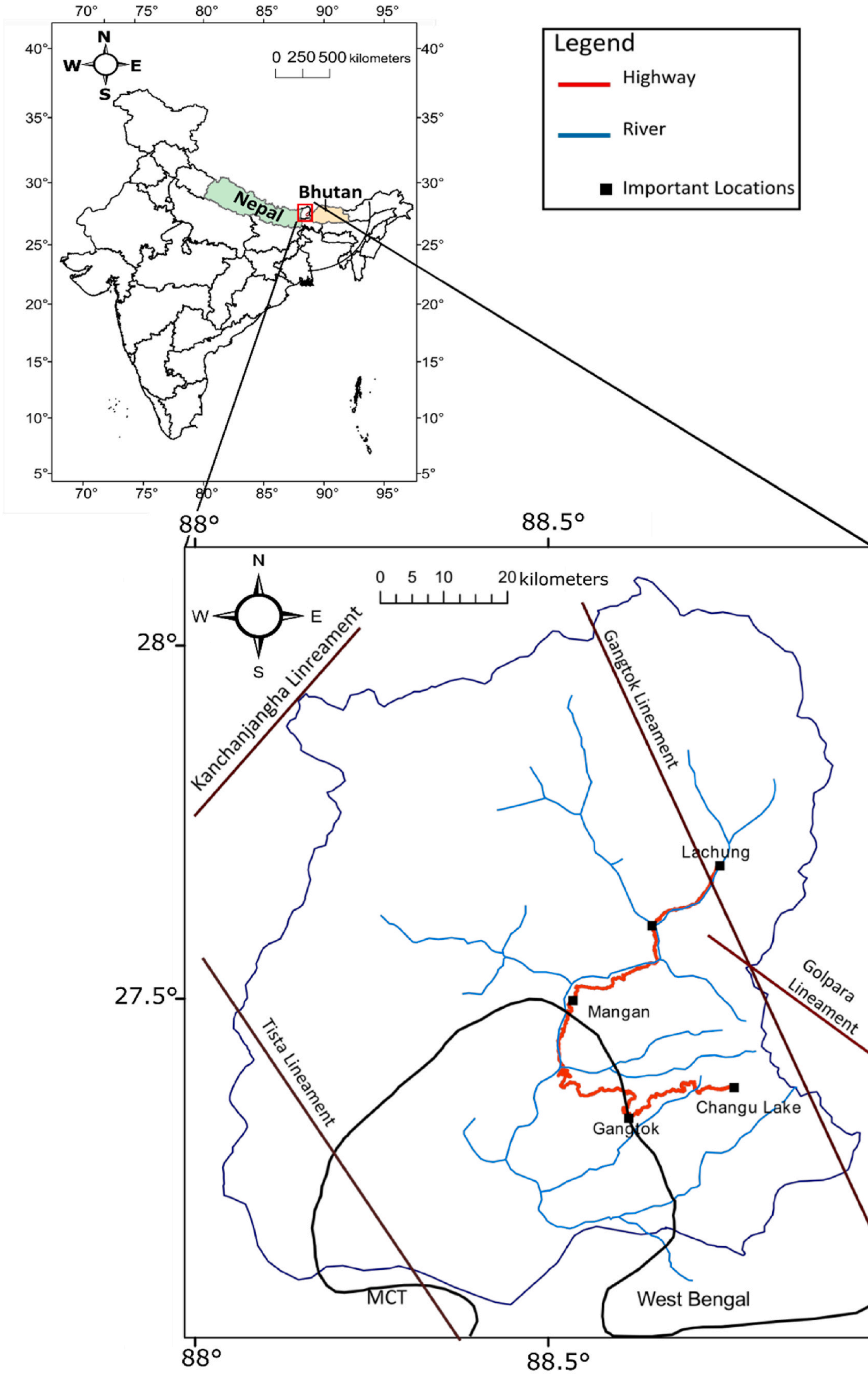

Fig. 3. The study area and location of the highway corridor.

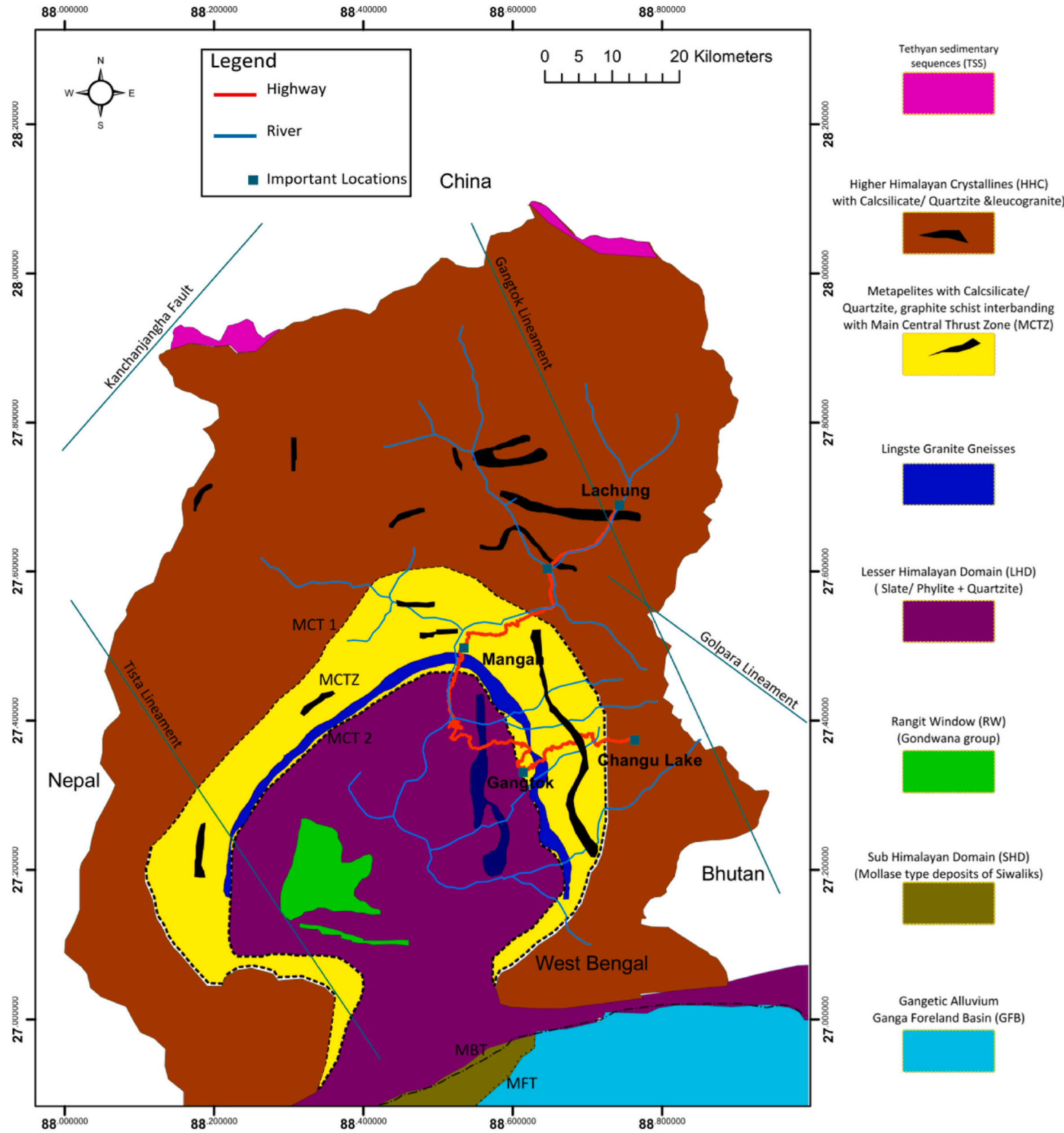

Fig. 4. Geological map of Sikkim showing major tectonic features (modified after Dasgupta et al., 2004 and Manglik et al., 2013).

of 787 earthquakes from the ISC catalogue, 301 earthquakes from USGS, and 132 earthquakes from other regional sources (GSI, IMD, Kolathayar et al., 2012, and Nath et al., 2017). Various types of magnitude scales are used to record the magnitude of an earthquake; i.e. surface-wave magnitude (M_s), body-wave magnitude (M_b), and local magnitude (M_l). Since these magnitude scales saturate at different higher magnitudes of an earthquake, which results in underestimation or overestimation of the size of an actual earthquake (Scordilis 2006). To eliminate this problem, the reported magnitude of the earthquakes are converted in moment magnitude (M_w), which do not saturate at higher magnitudes as it is calculated on the basis of the seismic moment (Hanks and Kanamori 1979), which is a function of the area of fault rupture and slip displacement occurred during an earthquake. The relationships defined by Scordilis (2006) are used to convert the earthquake magnitudes into moment magnitude (M_w).

3.1. Declustering of catalogue

In the Cornell–McGuire method of seismic hazard analysis, the earthquake occurrence is assumed to be an independent event and follows Poisson's distribution in time-space (Cornell 1968; McGuire 1976). Therefore, all the dependent events (foreshock and aftershock) must be excluded from the earthquake catalogue which will be used for further analysis. The removal of dependent events from an earthquake catalogue is known as declustering of the catalogue. Various algorithms for identifying and removing dependent events from an earthquake catalogue have been proposed over the years, such as Knopoff (1964), Knopoff and Gardner (1972), Gardner and Knopoff (1974), Reasenberg (1985), Zhuang et al. (2002) and Bottiglieri et al. (2009). The algorithm suggested by Gardner and Knopoff (1974) and Reasenberg (1985) is widely applied in the literature for declustering purposes. Gardner and Knopoff (1974) have used the windowing method, in which a time-space window based on the magnitude of an earthquake is selected to identify the dependent events. The declustering technique suggested by

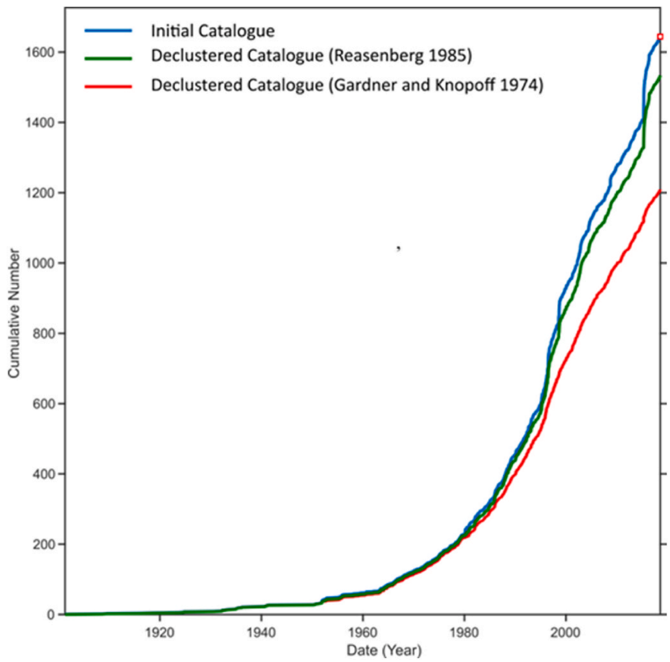

Fig. 5. Results of declustering by methods of Reasenberg (1985) and Gardner and Knopoff (1974). Cumulative number of Mw ≥ 4 earthquakes after declustering the initial catalogue.

Reasenberg (1985) uses a clustering method to identify dependent events. The earthquakes are linked to clusters based on the interaction zones defined in the space and the time domains. Omori's law (Utsu, 1961) is applied to define the temporal extent of the interaction zone. The spatial extent of the interaction zone is governed by the threshold of the magnitude of an earthquake (Molchan and Dmitrieva 1992) and is defined as

$$\log d(km) = 0.4M_o - 1.943 + k \tag{1}$$

where M_0 is earthquake magnitude and k is a spatial proximity parameter.

The largest event in the cluster is considered as mainshock and others are treated as dependent events. The methods suggested by Gardner and Knopoff (1974) and Reasenberg (1985) are applied in this study. The algorithm of Gardner and Knopoff (1974) removed 424 (25.8%) dependent events and resulted in 1220 independent events from the initial catalogue of 1644 events, whereas the algorithm of Reasenberg (1985) identified 1503 events as mainshocks and considered 141 (8.53%) seismic events as foreshocks and the aftershocks (Fig. 5). The outcomes of Van Stiphout et al. (2012) study suggests that the seismicity background obtained using the algorithm recommended by Gardner and Knopoff (1974), that follows a Poisson distribution. Hence, the declustered catalogue of 1220 events is further used for the calculation of seismic parameters.

3.2. Completeness analysis of catalogue

The magnitude of completeness (Mc) is described as the lowest magnitude at and above which all the seismic events in a spatial and temporal domain are recorded (Wiemer and Wyss 2000). It is vital to calculate the various levels of completeness of several sub-catalogues because if the incompleteness of the catalogue prepared for the long time interval is not considered, it would result in underestimation of the recurrence rates for small earthquakes. This is because large earthquakes are easy to record and they are usually complete for longer periods when compared with that of smaller magnitude earthquakes. Whereas, if the earthquake catalogue is prepared for a shorter time duration for which the lowest magnitude class incorporated in the computation is fully reported, mean rates of occurrence will not be reported correctly for the largest observed earthquakes. It is due to the lack of earthquake records of higher magnitudes due to their large recurrence interval (Stepp 1972). So, the seismicity parameters should be estimated incorporating the complete part of the earthquake catalogue. The completeness of the earthquake catalogue depends on the socio-economic condition, demographic variations, enhancement in the seismic event recording mechanism, and earthquake recording station coverage of the study area.

A method recommended by Stepp (1972) is used in this study to conduct the completeness analysis of the homogenized catalogue. The period of completeness for the homogenized catalogue for different intervals of magnitude are witnessed to be 4–4.5 for the period

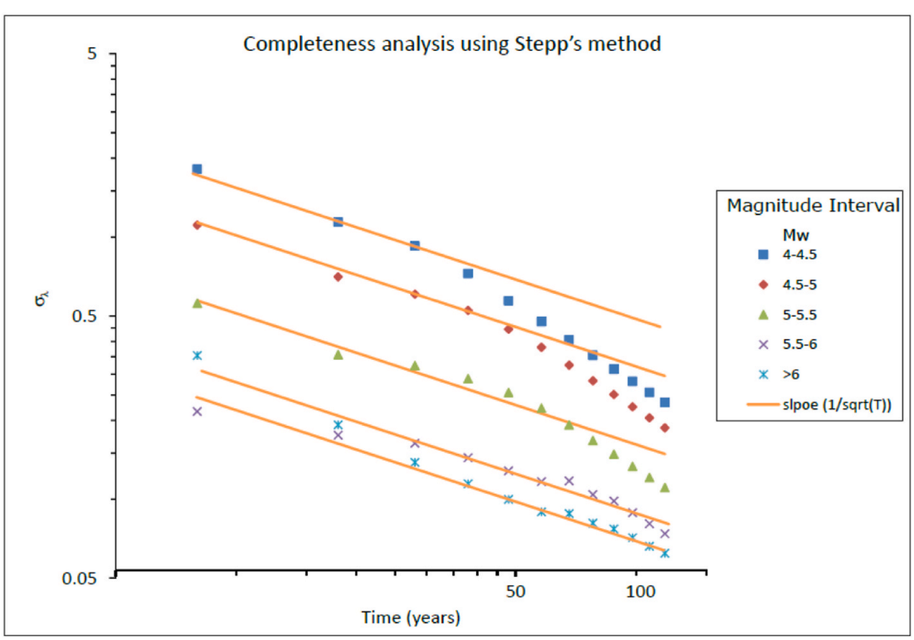

Fig. 6. Standard deviation of the average seismicity rate (σ_λ) of events as a function of sample length and magnitude class.

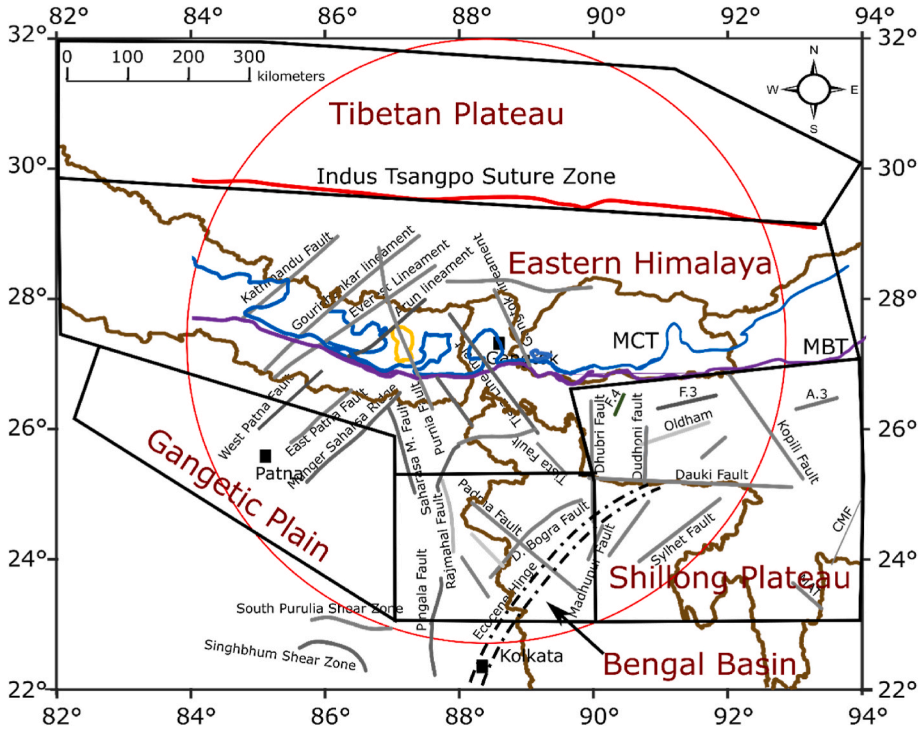

Fig. 7. Location and boundaries of considered seismic belts (Eastern Himalaya zone, Shillong Plateau Zone, Tibetan Plateau Zone and Bengal basin and Gangetic plain) in the study area with important tectonic structures.

1985–2018, 4.5–5 for 1970–2018, 5.0–5.5 for 1960–2018, 5.5–6 for 1910–2018, and magnitude greater than 6.0 for the periods 1900–2018 (Fig. 6). The periods of completeness for the lower magnitude ranges are observed to be smaller, because many smaller magnitude earthquakes may not get recorded in the past due to poor recording station coverage.

4. Seismic source zones and their seismicity parameters

4.1. Seismic source zones

To perform seismic hazard analysis, the demarcation of seismic source zones in the study area is an integral step. The seismic source zones can be demarcated as areas that share common seismological and tectonic properties taking into account that seismic sources in the area can be characterized by a distinct magnitude-frequency relationship (Thenhaus, 1986). This description suggests that the entire area in a particular source zone has the equal potential of generating an earthquake and in the future, earthquakes may trigger anywhere in the defined zone. For the present study, the areal seismic source zone is defined. To define areal seismic source zones, various tectonic features which include, faults and major lineaments are collected from the GSI map (GSI, 2000) and available literature and are plotted with earthquake distribution in the circular area of radius 500 km from Sikkim (Fig. 1). Considering the tectonic plate movement, historical seismicity, geology, and the earthquake distribution in the considered area, seismic sources are delineated at two levels. At first, the complete area is divided into five seismic belts naming the eastern Himalaya zone, Tibetan plateau zone, Shillong plateau zone, Bengal basin zone, and Gangetic plain zone (Fig. 7), further each seismic belt is divided into different areal seismic zones.

The Indian plate boundary within the study area is defined by a continental-continental collision segment in the north, and in the East, it is defined by complex to oblique subduction alongside the Burma-Andaman arc. The seismicity of the Eastern Himalayan zone and Tibetan plateau zone is related to the continental-continental collision of the Indian plate and Eurasian plate. The major tectonic features in the area are the MBT, the MCT, and the Indus Tsangpo Sature Zone (ITSZ). The ITSZ defines the northern boundaries of the Indian Plates. The area north of ITSZ is considered a Tibetan Plateau Zone. The eastern boundary of the Indian plate is delineated by the Burman- Andaman arc, along which an oblique convergence has been suggested (Fitch 1972; Curray et al., 1979) between the Indian and the Burmese plate. Shillong plateau zone and Bengal basin zone cover the prevailing region between the eastern Himalayan zone and Burmese arc, and the Himalayan fore-deep prevailing between stable Indian shield area and the Himalayas is considered as Gangetic plain zone.

4.1.1. Eastern Himalayan zone

The high seismicity of the eastern Himalayas is an adverse effect of continental–continental collision of the Indian plate and the Eurasian plate (Khattri and Tyagi 1983). 502 independent seismic events of magnitude $M_w \geq 4$ have been recorded in this zone during 1900–2018. In this region, the maximum recorded magnitude has been $M_w = 8$, which occurred at Bihar – Nepal border in 1934. The important seismogenic structures in this seismic belt are MCT and MBT and tectonic features like the Kathmandu fault, Tista fault, Gangtok lineament, Tista lineament, Arun lineament, and Everest lineament also contribute significantly to the seismicity of this belt. The mean focal depth calculated from the used earthquake catalogue in this zone is 33 km, whereas various studies reported that the majority of earthquakes in the Himalayas triggered at depths varying from 10 to 20 km (Priestley et al., 2008).

4.1.2. Tibetan Plateau Zone

Similar to the eastern Himalaya zone, the high seismicity of the Tibetan plateau zone is related to the collision of the Indian plate and Eurasian plate. Total count of 296 seismic events having magnitude $M_w \geq 4$ occurred in this belt with a maximum magnitude of 7.4. The mean focal depth of this seismic belt is 35 km and Bai et al. (2012) reported that the range of the focal depths varied from 0 to 40 km.

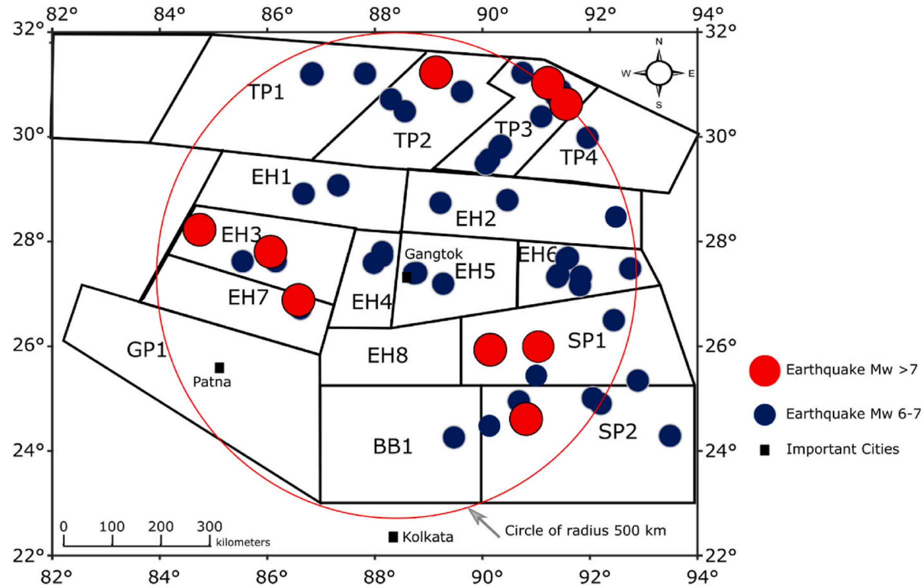

Fig. 8. Location and boundaries of areal seismic source zone considered for PSHA study plotted with important earthquake events and their epicenter location.

Table 1
Earthquake distribution in considered seismic belts.

Seismic Belt		Seismic Zone considered in each seismic belt	$M_w \geq 4$ (1900–2018)	M_{max} observed	a	b
Eastern Himalaya Zone	EZ	8 (EZ1, EZ2, EZ3, EZ4, EZ5,EZ6, EZ7, EZ8)	502	8 (1934)	5.328	0.65
Shillong Plateau Zone	SP	2 (SP1, SP2)	387	8.1 (1897) 7.2 (1918)	5.572	0.73
Tibetan Plateau Zone	TP	4 (TP1, TP2, TP3, TP4)	296	7.4 (1952)	5.227	0.68
Bengal basin and Gangetic plain	BB & GP	2 (BB1, GP1)	35	6.2 (1935)	4.902	0.80

4.1.3. Shillong Plateau Zone

This zone of high seismicity is situated between the eastern Himalaya zone and the Indo-Burmese arc subduction zone. This seismic belt is a distinct example of an "intraplate margin" region with active deformations (Nath and Thingbaijam 2011). In this seismic belt, 387 events ($M_w \geq 4$) are reported from 1897 to 2018 with a maximum magnitude of $M_w = 8.1$, which occurred on June 26, 1897. Prominent tectonic structures in this zone are Dauki Fault, Dhubri Fault, Dudhoni Fault, Sylhet Fault, and Kopili Fault. The mean focal depth of earthquakes triggered in this zone is 35 km.

4.1.4. Bengal basin zone

It is a zone of comparatively low seismicity, lies close to the Indo-Burmese subduction zone. More than 20 events of magnitude $M_w \geq 4$ triggered in this zone from 1900 to 2018 with an earthquake of maximum magnitude $M_w = 6.2$, experienced in 1935. The significant tectonic features of this zone are Eocene Hinge Zone (EHZ), Padma Fault, Madhupur Fault, Rajmahal Fault, Debagram-Bogra Fault, and Pingala Fault. The EHZ, which has a width of 25 km, is assumed to be the transition zone connecting continental crust and comparatively young oceanic crust which outspreads towards the Bay of Bengal (Curray et al., 1982). The average focal depth of this zone calculated from the used catalogue is 42 km.

4.1.5. Gangetic plain zone

The Gangetic plain, which is also recognized as the Himalayan fore-

Table 2
Seismic parameters of source zones considered in the present study.

Seismic Zone	β	SE β	λo	SE λo	Mmax obs	Mmax obs+0.5 (Gupta)	Mmax (Kijko)	SE Mmax	Mmax	Source Depth (km)
EZ1	1.79	0.22	2.086	0.414	6	6.5	6.4	0.27	6.5	10–30
EZ2	2.56	0.4	0.937	0.246	6.43	6.93	7.95	1.54	7.95	10–30
EZ3	2.07	0.13	2.605	0.449	7.8	8.3	8.3	0.2	8.3	10–30
EZ4	1.92	0.17	1.863	0.398	6.9	7.4	7.5	0.61	7.5	10–30
EZ5	1.8	0.32	0.995	0.259	6.5	7	7.1	0.59	7.1	10–30
EZ6	1.92	0.21	2.099	0.427	6.2	6.7	6.8	0.22	6.8	10–30
EZ7	1.72	0.53	0.371	0.126	8	8.5	8.5	0.2	8.5	10–30
EZ8	1.74	0.69	0.508	0.162	5.29	5.79	5.8	0.21	5.8	10–30
SP1	2.34	0.13	5.062	0.915	8.1	8.6	8.8	0.2	8.8	10–30
SP2	1.87	0.13	2.621	0.48	7.2	7.7	7.8	0.43	7.8	10–30
TB1	2.31	0.16	2.314	0.446	6.9	7.4	7.59	0.72	7.59	10–30
TB2	2.67	0.24	2.401	0.476	7.2	7.7	8	0.1	8	10–30
TB3	1.8	0.23	1.12	0.257	7.4	7.9	8.5	1.4	8.5	10–30
TB4	2.13	0.48	0.583	0.171	6.1	6.6	6.8	0.69	6.8	10–30
BB1	2.07	0.21	0.601	0.191	6.22	6.72	6.6	0.57	6.72	10–30
GP1	2.23	0.22	0.451	0.167	5.9	6.4	6.5	1.2	6.5	10–30

SE = Standard Error, M_{maxobs} = Maximum observed earthquake in seismic zone.

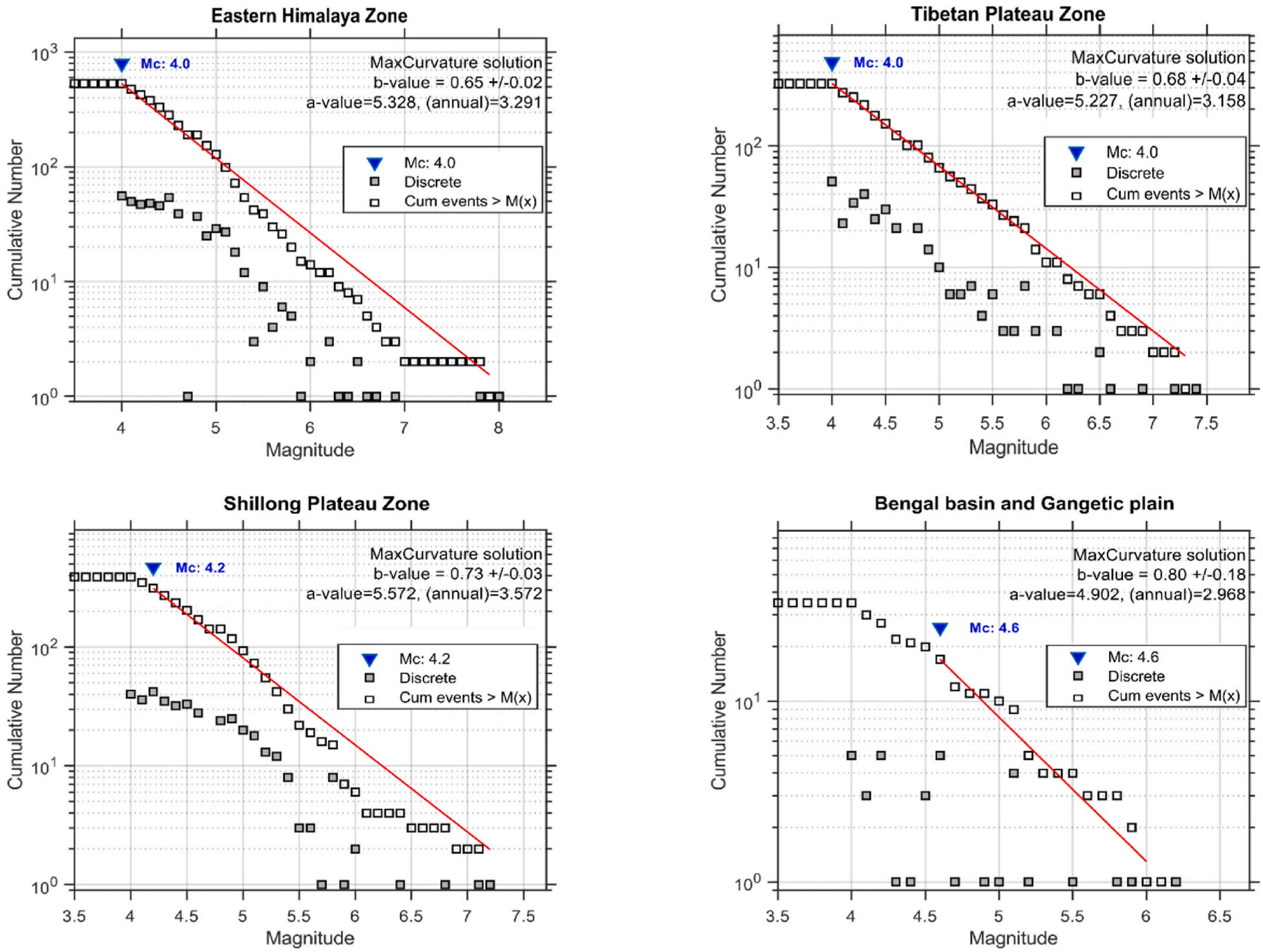

Fig. 9a. Cumulative and non-cumulative (discrete) FMD of the earthquakes of considered (a) seismic belts

deep prevailing between the stable Indian shield area and the Himalayas. Seismic activity in this region is less when compared to the seismicity of Himalayas (Quittmeyer and Jacob 1979). The seismicity of the Gangetic plain is mainly related to strike-slip faulting (Gupta 2006). East Patna fault, West Patna fault, and Munger Saharasa Ridge are major tectonic structures of this zone.

For achieving a more clear perspective of the spatial and temporal disparities of seismic activities of the study area, each seismic belt is further divided into different areal seismic zones (Fig. 8) (Table 1). Different seismic zones inside a seismic belt are defined depending upon the variation of seismic activity in terms of focal depth and magnitude and clustering of earthquakes from the catalogue surrounding the important geological and tectonic features. Previous contributions of Bhatia et al. (1999), Zhang et al. (1999), Gupta (2006), and Kolathayar and Sitharam (2012) have also been utilized for defining the boundaries of seismic belts and areal seismic zones in the study area.

4.2. Seismic parameters of seismic zones

Average seismicity at threshold magnitude (λ_o), maximum earthquake potential (M_{max}), “b-value” defined by Gutenberg and Richter (1944), and focal depth are the various parameters required to define the seismicity of the seismic source zone. The above-mentioned parameters are estimated for all the seismic source zones (Table 2). For a seismic source zone Frequency Magnitude Distribution (FMD) of earthquakes is assumed to be under the Gutenberg–Richter (G–R) relation (Gutenberg and Richter 1944) stated as,

$$\log(N) = a - b(M) \tag{2}$$

where N is the number of seismic events having a magnitude greater than M, a and b are the seismicity parameters of the concerned region, ‘a’ value is a measure of seismicity of the region, whereas ‘b’ value represents the relative number of small and large earthquakes. A lower b-value indicates that the frequency of high magnitude earthquakes is high and vice-versa. To compare the seismicity of the considered seismic belt, parameters ‘a’ and ‘b’ defined by the G-R relationship (Gutenberg and Richter 1944) are calculated for each seismic belt using MATLAB (2018) based tool ZMAP (Wiemer 2001) (Table 1). Plots of cumulative and non-cumulative (discrete) FMD for the earthquake catalogue of each considered seismic belt and their seismic zones are shown in Fig. 9a and b. The FMD of seismic source zone EZ8, BB1 and GP1are not shown due to less number earthquakes in the seismic zone.

Seismic parameters are estimated by incorporating the incompleteness of the earthquake catalogue. This purpose is achieved by the preparation of sub-catalogues for each seismic zone and these sub-catalogues are complete to the different threshold of magnitude. To calculate the earthquake magnitude exceedance rates, the seismic activity of the areal seismic source zone is modelled as Modified Gutenberg–Richter (MGR)–Poisson model. The seismicity, with the help of this model, is represented as (Cornell and Vanmarcke, 1969).

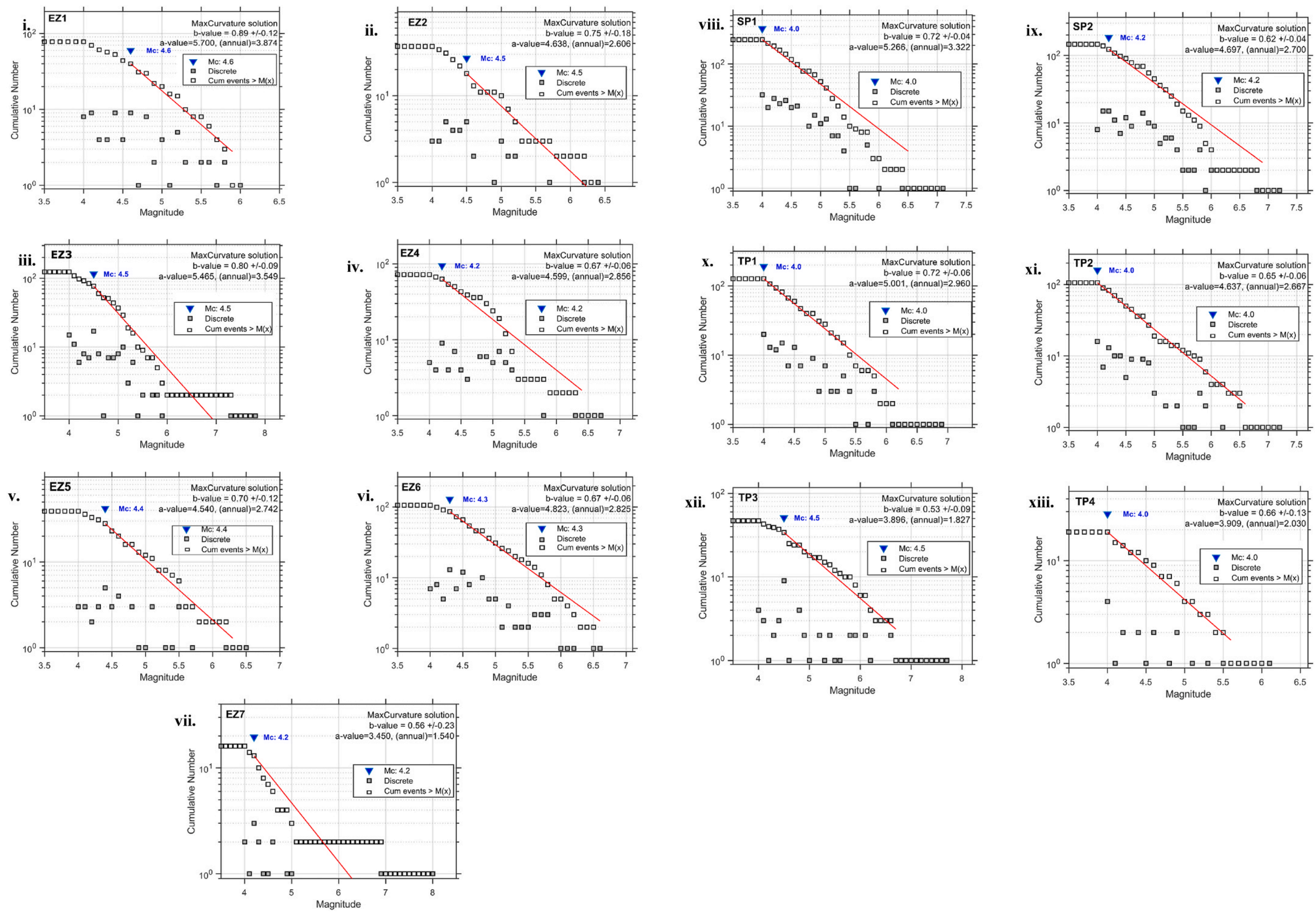

Fig. 9b. Cumulative and non-cumulative (discrete) FMD of the earthquakes of considered seismic zones.

$$\lambda(M) = \lambda_o \frac{\exp(-\beta M) - \exp(-\beta M_{\max})}{\exp(-\beta M_o) - \exp(-\beta M_{\max})} \tag{3}$$

$Mo \leq M \leq Mmax$

where β represents a seismic parameter comparable to the 'b' of the G-R relationship (β = 2.303b), *o* is the mean rate of seismic activity having a threshold magnitude, M_0 (here, M_0 = 4.0), and M_{max} is the maximum possible earthquake magnitude. For this study, M_{max} is calculated utilizing two methods, the Bayesian extension of the K–S–B estimator (Kijko 2004) and the incremental method suggested by Gupta (2006). A MATLAB-based code (HA3) developed by Kijko et al. (2016) is used to estimate M_{max}. The Gutenberg–Richter b value and λ_0 for each source zone is calculated by utilizing the joint likelihood function suggested by Kijko et al. (2016). The incompleteness of the earthquake catalogue and the variation of seismicity with time are considered for 'b' value estimation in this new method. In the incremental approach of M_{max} calculation suggested by Gupta (2006), the recorded maximum magnitude in the concerned seismic source zone is increased by 0.5 units. This method is simple and implemented by several researchers in seismic hazard assessment studies (Bahuguna and Sil, 2020; Bashir and Basu, 2018). The maximum value obtained out of these two methods is further used for hazard analysis related calculations.

5. Selection of ground motion attenuation relationships

Ground motion attenuation relationships are very critical in the assessment of seismic hazards (Crowley et al., 2005). Even though the methodology and framework of PSHA are well established, the selection of attenuation relationships to predict the ground motion at the sites of concern is still a challenging task for researchers. The ground motion attenuation relationships are selected depending upon the seismotectonic region, the magnitude of earthquakes, distance, range of period, regional wave propagation characteristics, and capability to model site effects (Silva et al., 2014). The seismotectonic of the concerned study area is complex. The Himalayan region and Tibetan plateau region are considered as active shallow crust regimes whereas the Shillong plateau zone is an example of an intraplate margin of high deformation (Nath and Thingbaijam 2012). Most of the earthquakes of catalogue triggered at a depth varying from 10 km to 40 km with an average earthquake depth of 30 km.

The Himalayan region's attenuation behaviour, employing the available ground motion data have been studied by several researchers previously. Using both observed and simulated earthquake data, the regional GMPEs have been derived (Nath et al., 2009; Baruah et al., 2009; Sharma et al., 2009; Gupta 2010; NDMA 2010; Anbazhagan et al., 2013) with limited observed ground motions due to lack of strong-motion records. Further, other GMPEs developed for analogous tectonic conditions with a comparatively larger set of recorded ground motion can also be valid in the Himalayan region. The selection of appropriate GMPEs from several available GMPEs (Douglas 2011) has been done based on previous recommendations for selection of ground motion attenuation relationships (Cotton et al., 2006; Bommer et al., 2010), 7 GMPEs (Atkinson and Boore 2006; Zhao et al., 2006; Abrahamson and Silva 2008; Boore and Atkinson 2008; Campbell and Bozorgnia 2008; Chiou and Youngs 2008; Akkar and Bommer 2010) are

Table 3
PGA (g) for 10% PoE in the 50-years, i.e., the RP of 474.6-years.

Site	AS-08	BA-08	CB-08	CY-08	Mean hazard
Gangtok	0.31	0.20	0.16	0.38	0.274
Yumthang	0.30	0.19	0.15	0.34	0.26
Mangan	0.33	0.22	0.17	0.39	0.29
Tsomgo Lake	0.29	0.19	0.15	0.33	0.25

AS-08 = Abrahamson and Silva (2008), **BA-08** = Boore and Atkinson (2008). **CB-08** = Campbell and Bozorgnia (2008), **CY-08** = Chiou and Youngs (2008).

Table 4
PGA (g) for 40% PoE in the 50-years, i.e., the RP of 97.9-years.

Site	AS-08	BA-08	CB-08	CY-08	Mean hazard
Gangtok	0.16	0.10	0.09	0.183	0.137
Yumthang	0.15	0.10	0.08	0.17	0.13
Mangan	0.17	0.10	0.10	0.20	0.15
Tsomgo Lake	0.15	0.09	0.085	0.17	0.13

Table 5
PGA (g) for 2% PoE in the 50-years, i.e., the RP of 2474.9-years.

Site	AS-08	BA-08	CB-08	CY-08	Mean hazard
Gangtok	0.53	0.40	0.26	0.64	0.50
Yumthang	0.51	0.39	0.25	0.61	0.48
Mangan	0.56	0.44	0.28	0.68	0.535
Tsomgo Lake	0.50	0.37	0.245	0.59	0.464

found to be applicable in the study area.

The efficacy test, a quantitative suitability test is an information-theoretic model based on the calculation of average sample log-likelihood (LLH) is recommended by Scherbaum et al. (2009) for the ranking of GMPEs and has been successfully employed by Delavaud et al. (2009). Nath and Thingbaijam (2011) suggested a set of GMPEs for various seismotectonic environments prevailing in India by applying the efficacy test of Scherbaum et al. (2009). Further, the efficacy test of GMPEs has been performed considering the Macroseismic Intensity Map of the Nepal earthquake (1803) (Anbazhagan et al., 2017) and by using the macroseismic intensity map (1833) and Bihar–Nepal earthquake (1934) (Anbazhagan et al., 2019). Considering the suggestion of ground motion attenuation relationships for active shallow crust regime (Stewart et al., 2015) along with several efficacy test results of GMPEs (Nath and Thingbaijam 2011; Anbazhagan et al. 2017, 2019), the next generation attenuation relationship suggested by Abrahamson and Silva (2008), Boore and Atkinson (2008), Campbell and Bozorgnia (2008) and Chiou and Youngs (2008) are selected from the list of seven GMPEs applicable in the study area. An equal weighting factor of 25% has been assigned for each of these GMPE in the calculation of PGA.

6. PSHA results

All the calculations related to the hazard analysis are done using the ''EZ-FRISK'' software (Version 7.65), that uses the approach suggested by Cornell–McGuire (Cornell 1968; McGuire 1976). The obtained ground acceleration results correspond to the bedrock site condition. The hazard calculation has been done for the grid of sites spaced 0.05° and PGA is estimated at the central point of each grid cell. All the seismic sources in a circular region of radius 300 km around the central point of each grid cell are considered, to calculate the PGA values. The calculation of the seismic hazard parameter is done by disaggregating the magnitude range into incremental values of 0.1 and the focal depth into 1 km intervals. From the present PSHA study, the PGA value of 10%, 40%, and 2% PoE in 50-years, obtained at four important locations on the highways (Gangtok, Yumthang, Mangan, and Tsomgo Lake) are shown in Tables 3–5. The maximum PGA is obtained from the attenuation relationship proposed by Chiou and Youngs (2008) for various values of PoE (2%, 10%, and 40%) in 50-years. The lowest PGA is obtained by using the attenuation model developed by Campbell and Bozorgnia (2008). The sensitivity of the total hazard curve to the

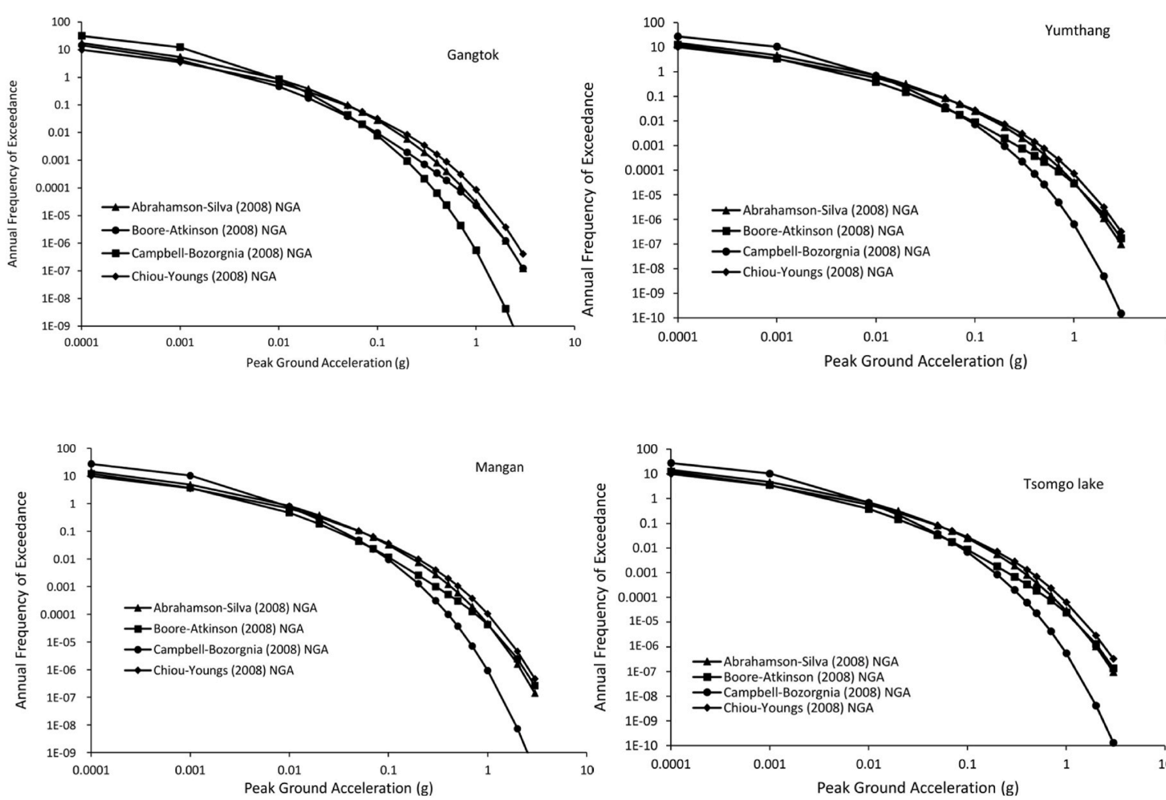

Fig. 10. The sensitivity of the total hazard curve to the attenuation relationships for Gangtok, Yumthang, Mangan, and Tsomgo Lake.

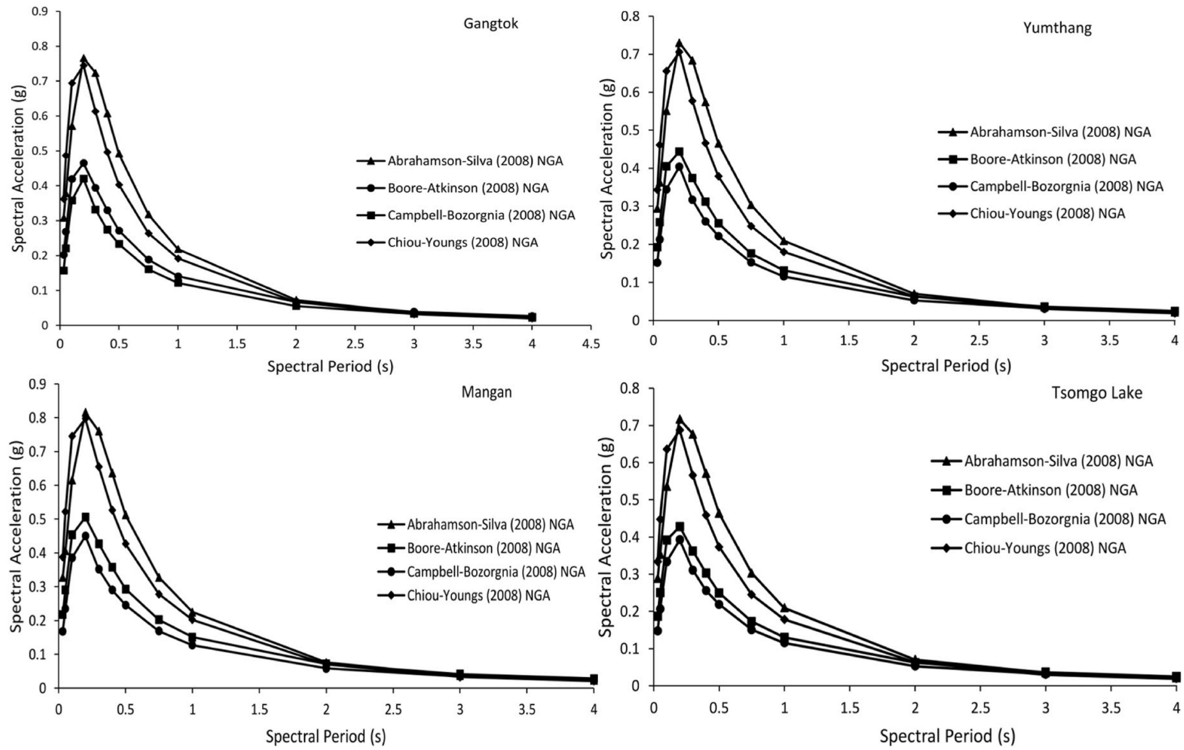

Fig. 11. The sensitivity of the UHS to the attenuation relationships for a RP of 474.6-years for Gangtok, Yumthang, Mangan, and Tsomgo Lake.

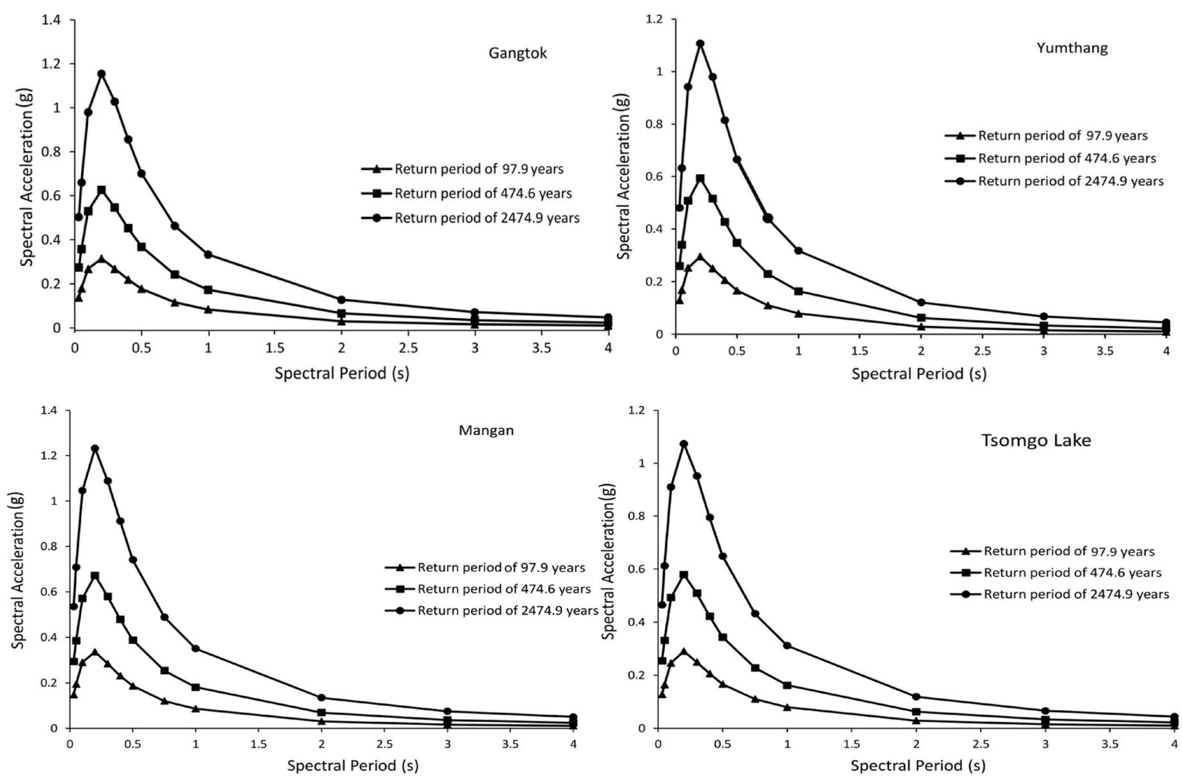

Fig. 12. The UHS for RPs of 97.9-years, 474.6-years, and 2474.9-years of Gangtok, Yumthang, Mangan, and Tsomgo Lake.

attenuation relationships is shown in Fig. 10 for PGA. The sensitivity of the UHS for the RP of 474.6-years to the attenuation relationships is shown in Fig. 11. The UHS of Gangtok, Yumthang, Mangan, and Tsomgo Lake for RPs 97.9-years, 474.6-years, and 2474.9-years is shown in Fig. 12. PGA contour map obtained after assigning equal weightage to four used GMPEs for a 10% PoE in 50-years and 40% PoE in 50-years is plotted along the highway (Fig. 13 and Fig. 14), to identify the critical sections based on the ground acceleration parameter. The PGA values obtained for the study area vary from 0.12 to 0.18g for the 97.9-year RP, 0.24–0.36g for the 474.6-year RP, and 0.46–0.54g for the 2474.9-year

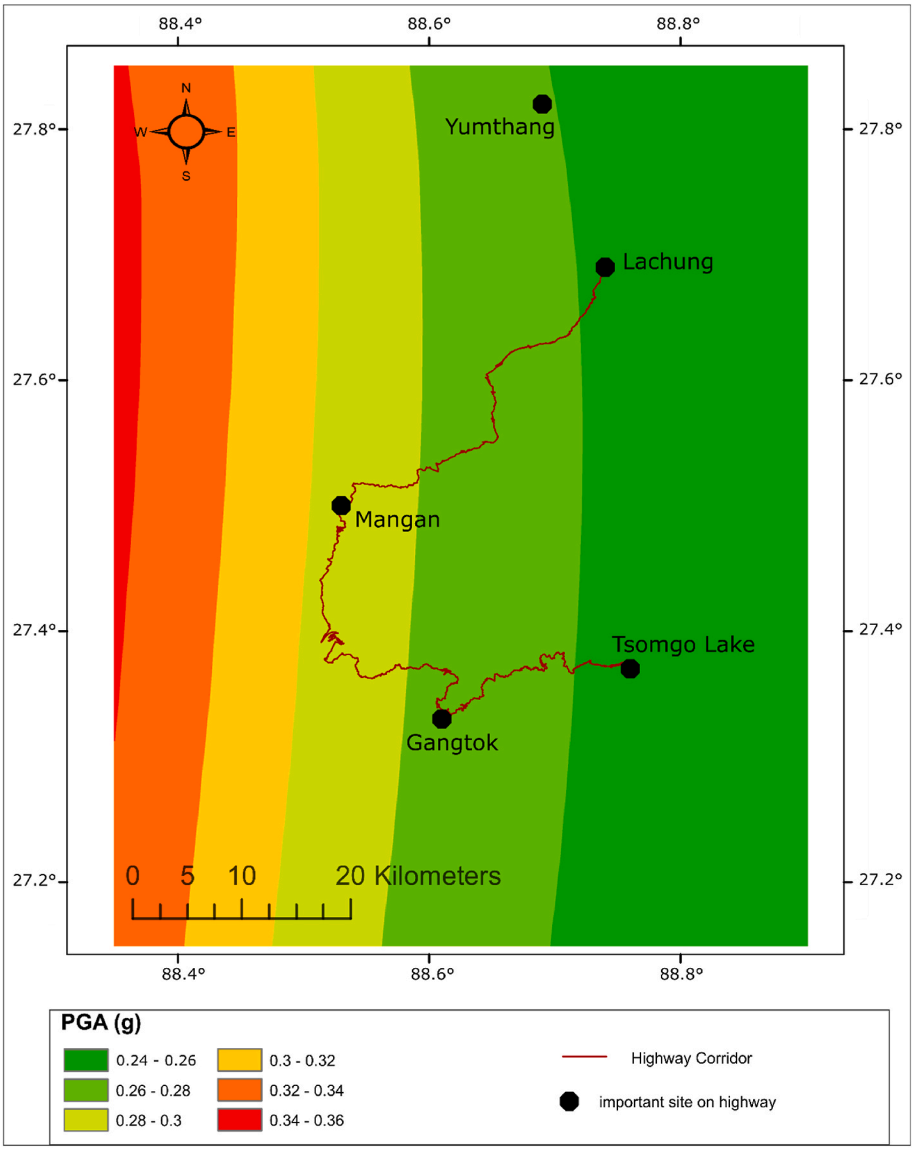

Fig. 13. The PGA hazard map for a 10% PoE in 50-years along the highways.

RP. The PGA value obtained for Gangtok in the present study for a 10% PoE in 50-years has been compared with the results of several earlier probabilistic seismic hazard studies (Table 6). Bhatia et al., (1999), NDMA (2010) and Nath and Thingbaijam (2012) reported the probabilistic hazard map of the entire country. Bhatia et al., (1999) in their study used a single GMPE of Joyner and Boore (1981) for the whole country and computed seismic hazard at grided locations with 0.5° × 0.5° resolution. Nath and Thingbaijam (2012), in their study, used 4–5 GMPEs based on different seismotectonic regions and styles of faulting and assigned equal weightage to all the selected GMPEs, and calculated PGA on a grid-point scale at a resolution of 0.2° of the entire study region. Whereas, NDMA (2010) has reported the seismic hazard map of the country considering the GMPE developed from the simulated ground motions and PGA calculation has been done for a grid spaced at 0.2°. Das et al., (2016) presented the PGA map of the North Eastern region of India employing two GMPEs of Gupta (2010) and Boore and Atkinson (2008) and estimated the PGA at a grid spacing of 0.1° × 0.1° extended over the North-East region of India. The hazard calculation in the present study has been done for a grid spaced at 0.05°, using four next-generation attenuation relationships.

The response spectra obtained at Gangtok after the PSHA study is compared with the 5% damped acceleration response spectra of the recorded acceleration time history at Gangtok during the 2011 (M_w = 6.9) Sikkim earthquake. The response spectra obtained after the present study is also compared with the Indian seismic code-specified response spectra for a rock site (Fig. 15). A straight comparison of UHS obtained through the PSHA study with observed ground motion in the study area is not reasonable. Though when normalized by corresponding PGA, the shape of hazard spectra should be similar to that of observed ground motion. It is evident from Fig. 15, the shape of uniform hazard spectra obtained in the present study is similar to the recorded ground motion spectra of the 2011 Sikkim earthquake. It may be noted from Fig. 15 that up to spectral period 0.15s, the normalized spectral acceleration values obtained from the PSHA study at Gangtok are more than the Indian Standard (IS) code value as well as 2011 earthquake recorded spectra, from spectral period 0.2s–0.5s normalized spectral acceleration of 2011 earthquake spectra is very high as compared to the IS code spectra and response spectra obtained for Gangtok site. For a spectral period of more than 1.3s, recorded ground motion response spectra are matching with the calculated response spectra of Gangtok. The IS code response spectra are conservative for spectral acceleration at a period higher than 0.5s. The higher normalized spectral acceleration values observed at the short

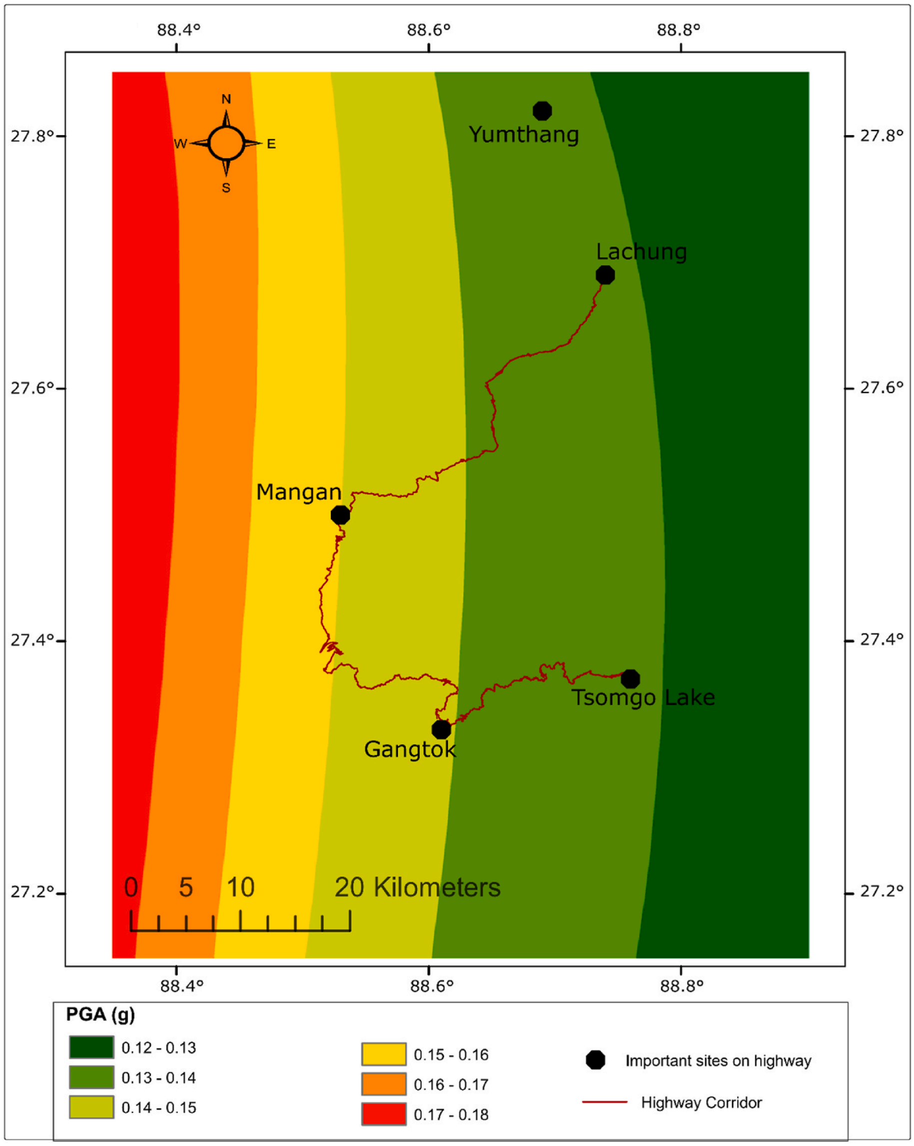

Fig. 14. The PGA hazard map for a 40% PoE in 50-years along the highways.

Table 6
Comparison of PGA (g) values calculated in this study and reported by other studies for Gangtok corresponding to 10% PoE in 50-years.

Study	PGA(g)
Present Study	0.274
GSHAP (Bhatia et al., 1999)	0.25
BIS(2002) for MCE	0.24
NDMA 2010 (Iyengar et al., 2010)	0.18
Nath and Thingbaijam (2012)	0.50
Das et al. (2016)	0.146

period region of obtained hazard spectra is because this part of the spectrum is governed by small to moderate nearby earthquakes and this observation is in coherence with the result of hazard deaggregation analysis (Fig. 16 and Fig. 17).

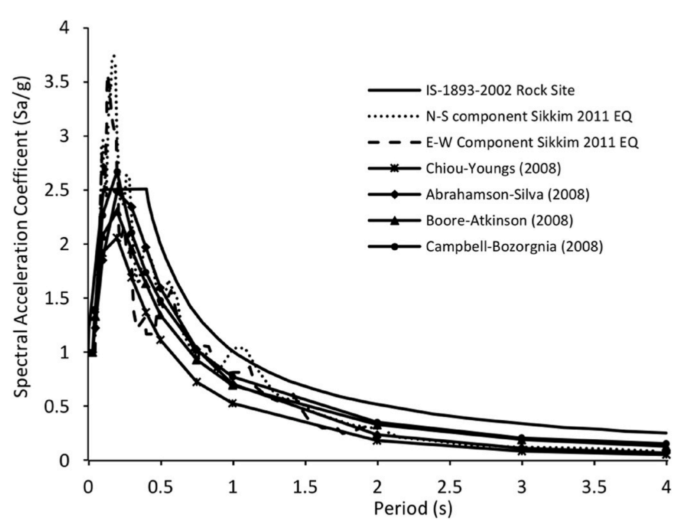

Fig. 15. Comparison of normalized acceleration response spectra.

7. Conclusion

The objective of this study is to do a PSHA analysis of highway corridors in Sikkim in order to determine input ground motions for earthquake-triggered landslide hazard assessment. For this purpose, the

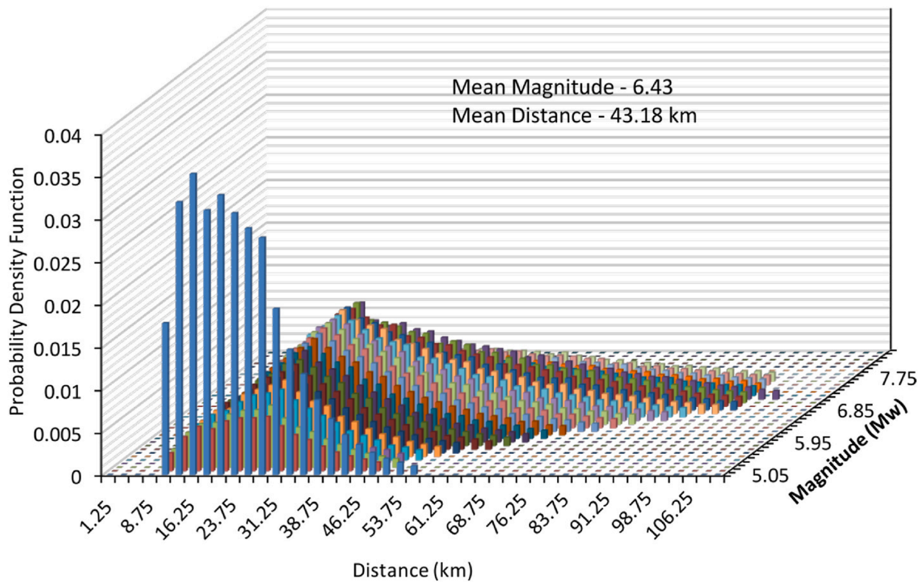

Fig. 16. Hazard deaggregation curve of Gangtok for a RP of 474.6-years.

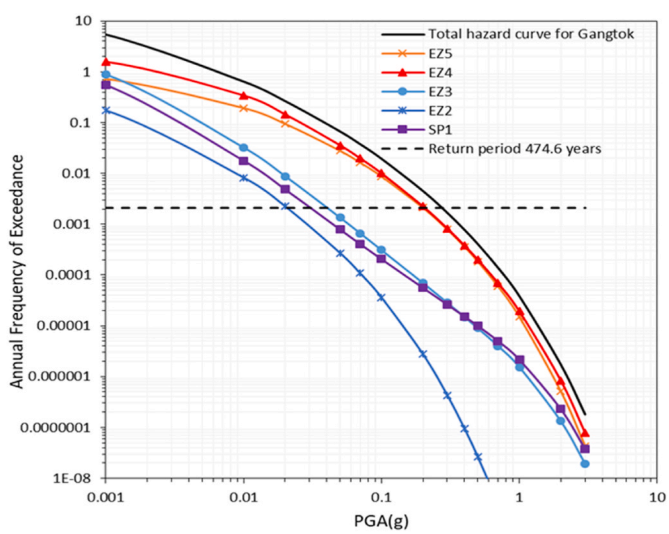

Fig. 17. Hazard curve for 5 most contributing seismic sources at Gangtok.

updated earthquake catalogue and widely used GMPEs developed for similar tectonic regions have been utilized. With concern to local variations of tectonic activities, the complete area is parted into 16 seismic source zones and the seismicity parameters of such zones have been estimated using the recent methodology (Kijko et al., 2016). The PGA maps have been prepared for bedrock site conditions and observed a notable variation in the obtained PGA values in the study area contrary to the uniform PGA value recommended by the Indian standard seismic code (IS code 1893–2002). The PGA values obtained for the study area varies from 0.12 to 0.18g for the 97.9-year RP, 0.24–0.36g for the 474.6-year RP, and 0.46–0.54g for the 2474.9-year RP. The hazard spectra obtained from this study will be further used to generate ground motions utilizing the spectral matching technique. The PGA map of the study area will be useful for the assessment of earthquake-triggered landslide hazards at the regional scale.

Author statement

Saurav Kumar: Formal analysis, Methodology, Writing- Original draft preparation. **Aniruddha Sengupta:** Supervision, Resources, Writing - Review & Editing, Funding acquisition. **Reginald Hermanns, John Dehls, Rajinder Kr. Bhasin, Ivanna Penna, Vikram Gupta:** Review & Editing, Funding acquisition.

Declaration of competing interest

The authors declare that they have no known competing financial interests or personal relationships that could have appeared to influence the work reported in this paper.

Acknowledgements

The financial support by the Ministry of Earth Sciences (MoES), Govt of India (GoI), New Delhi, with Sanction No. MoES/Indo-Nor/PS-2/2015 dtd April 26, 2017 is duly acknowledged.

References

Abdulnaby, W., Onur, T., Gök, R., Shakir, A.M., Mahdi, H., Al-Shukri, H., Ramthan, A., 2020. Probabilistic seismic hazard assessment for Iraq. J. Seismol. 24, 595–611.
Abrahamson, N., Silva, W., 2008. Summary of the Abrahamson & Silva NGA ground-motion relations. Earthq. Spectra 24 (1), 67–97.
Acharyya, S.K., 1989. The Daling Group, its nomenclature, tectono-stratigraphy and structural grain: with notes on their possible equivalents. Visesa Prakasana-Bharatiya Bhuvaijñanika Sarveksana (22), 5–13.
Acharyya, S.K., 1992. Tectonics of eastern Himalaya, its concealed tertiary foreland basin and the nature of northeastern orographic bend. In: Proc. Symp. Him. Geol. Sem., Shimane, Japan.
Akkar, S., Bommer, J.J., 2010. Empirical equations for the prediction of PGA, PGV, and spectral accelerations in Europe, the Mediterranean region, and the Middle East. Seismol Res. Lett. 81 (2), 195–206.
Anbazhagan, P., Bajaj, K., Dutta, N., Moustafa, S.S., Al-Arifi, N.S., 2017. Region-specific deterministic and probabilistic seismic hazard analysis of Kanpur city. J. Earth Syst. Sci. 126 (1), 12.
Anbazhagan, P., Bajaj, K., Matharu, K., Moustafa, S.S., Al-Arifi, N.S., 2019. Probabilistic seismic hazard analysis using the logic tree approach–Patna district (India). Nat. Hazards Earth Syst. Sci. 19 (10), 2097–2115.
Anbazhagan, P., Kumar, A., Sitharam, T.G., 2013. Ground motion prediction equation considering combined dataset of recorded and simulated ground motions. Soil Dynam. Earthq. Eng. 53, 92–108.
Atkinson, G.M., Boore, D.M., 2006. Earthquake ground-motion prediction equations for eastern North America. Bull. Seismol. Soc. Am. 96 (6), 2181–2205.
Bahuguna, A., Sil, A., 2020. Comprehensive seismicity, seismic sources and seismic hazard assessment of Assam, North East India. J. Earthq. Eng. 24 (2), 254–297.
Bai, L., Ritsema, J., Zhao, J., 2012. Focal depth estimates of earthquakes in the Himalayan-Tibetan region from teleseismic waveform modeling. Earthq. Sci. 25 (5–6), 459–468.
Baker, J.W., 2008. An Introduction to Probabilistic Seismic Hazard Analysis (PSHA), 1, p. 72. White paper, version.

Baruah, S., Baruah, S., Gogoi, N.K., Erteleva, O., Aptikaev, F., Kayal, J.R., 2009. Ground motion parameters of Shillong plateau: one of the most seismically active zones of northeastern India. Earthq. Sci. 22 (3), 283–291.
Bashir, A., Basu, D., 2018. Revisiting probabilistic seismic hazard analysis of Gujarat: an assessment of Indian design spectra. Nat. Hazards 91 (3), 1127–1164.
Bhatia, S.C., Kumar, M.R., Gupta, H.K., 1999. A Probabilistic Seismic Hazard Map of India and Adjoining Regions.
BIS, 2002. IS 1893–2002, Indian Standard Criteria for Earthquake Resistant Design of Structures, Part 1—general Provisions and Buildings. Bureau of Indian Standards, New Delhi.
Bommer, J.J., 2002. Deterministic vs. probabilistic seismic hazard assessment: an exaggerated and obstructive dichotomy. J. Earthq. Eng. 6 (1), 43–73.
Bommer, J.J., Douglas, J., Scherbaum, F., Cotton, F., Bungum, H., Fäh, D., 2010. On the selection of ground-motion prediction equations for seismic hazard analysis. Seismol Res. Lett. 81 (5), 783–793.
Boore, D.M., Atkinson, G.M., 2008. Ground-motion prediction equations for the average horizontal component of PGA, PGV, and 5%-damped PSA at spectral periods between 0.01 s and 10.0 s. Earthq. Spectra 24 (1), 99–138.
Bottiglieri, M., Lippiello, E., Godano, C., De Arcangelis, L., 2009. Identification and spatiotemporal organization of aftershocks. J. Geophys. Res. Solid Earth 114 (B3).
Campbell, K.W., Bozorgnia, Y., 2008. NGA ground motion model for the geometric mean horizontal component of PGA, PGV, PGD and 5% damped linear elastic response spectra for periods ranging from 0.01 to 10 s. Earthq. Spectra 24 (1), 139–171.
Chiou, B.J., Youngs, R.R., 2008. An NGA model for the average horizontal component of peak ground motion and response spectra. Earthq. Spectra 24 (1), 173–215.
Corigliano, M., Lai, C.G., Menon, A., Ornthammarath, T., 2012. Seismic input at the archaeological site of Kancheepuram in Southern India. Nat. Hazards 63 (2), 845–866.
Cornell, C.A., 1968. Engineering seismic risk analysis. Bull. Seismol. Soc. Am. 58 (5), 1583–1606.
Cornell, C.A., Vanmarcke, E.H., 1969, January. The major influences on seismic risk. In: Proceedings of the Fourth World Conference on Earthquake Engineering, 1, pp. 69–83.
Cotton, F., Scherbaum, F., Bommer, J.J., Bungum, H., 2006. Criteria for selecting and adjusting ground-motion models for specific target regions: application to central Europe and rock sites. J. Seismol. 10 (2), 137–156.
Crowley, H., Bommer, J.J., Pinho, R., Bird, J., 2005. The impact of epistemic uncertainty on an earthquake loss model. Earthq. Eng. Struct. Dynam. 34 (14), 1653–1685.
Curray, J.R., Emmel, F.J., Moore, D.G., Raitt, R.W., 1982. Structure, tectonics, and geological history of the northeastern Indian Ocean. In: The Ocean Basins and Margins. Springer, Boston, MA, pp. 399–450.
Curray, J.R., Moore, D.G., Lawver, L.A., Emmel, F.J., Raitt, R.W., Henry, M., Kieckhefer, R., 1979. Tectonics of the Andaman Sea and Burma: Convergent Margins.
Das, R., Sharma, M.L., Wason, H.R., 2016. Probabilistic seismic hazard assessment for northeast India region. Pure Appl. Geophys. 173 (8), 2653–2670.
Dasgupta, S., Ganguly, J., Neogi, S., 2004. Inverted metamorphic sequence in the Sikkim Himalayas: crystallization history, P–T gradient and implications. J. Metamorph. Geol. 22 (5), 395–412.
Delavaud, E., Scherbaum, F., Kuehn, N., Riggelsen, C., 2009. Information-theoretic selection of ground-motion prediction equations for seismic hazard analysis: an applicability study using Californian data. Bull. Seismol. Soc. Am. 99 (6), 3248–3263.
Douglas, J., 2011. Ground-motion Prediction Equations 1964-2010. PEER Report 2011/102, Pacific Earthquake Engineering Research Center. College of Engineering. University of California, Berkeley.
Fitch, T.J., 1972. Plate convergence, transcurrent faults, and internal deformation adjacent to southeast Asia and the western Pacific. J. Geophys. Res. 77 (23), 4432–4460.
Fugro Consultants Inc, 2014. EZ-FRISK 7.65: Software for Earthquake Ground Motion Estimation (User's Manual). Risk Engineering, Inc., New York.
Gansser, A., 1964. Geology of the Himalayas.
Gardner, J.K., Knopoff, L., 1974. Is the sequence of earthquakes in Southern California, with aftershocks removed, Poissonian? Bull. Seismol. Soc. Am. 64 (5), 1363–1367.
Geological Survey of India (https://www.gsi.gov.in/).
Ghosh, S., Chakraborty, I., Bhattacharya, D., Bora, A., Kumar, A., 2012. Generating field-based inventory of earthquake-induced landslides in the Himalayas-an aftermath of the 18 September 2011 Sikkim Earthquake. Indian J. Geosci. 66 (1), 27–38.
Godt, J.W., Baum, R.L., Savage, W.Z., Salciarini, D., Schulz, W.H., Harp, E.L., 2008. Transient deterministic shallow landslide modeling: requirements for susceptibility and hazard assessments in a GIS framework. Eng. Geol. 102 (3–4), 214–226.
GSI (Geological Survey of India), 2000. Seismotectonic Atlas of India and its Environs.
Guha, S.K., 1962. Seismic regionalization of India. In: Proceedings of Second Symposium on Earthquake Engineering, pp. 191–207.
Gupta, I.D., 2006. Delineation of probable seismic sources in India and neighbourhood by a comprehensive analysis of seismotectonic characteristics of the region. Soil Dynam. Earthq. Eng. 26 (8), 766–790.
Gupta, I.D., 2010. Response spectral attenuation relations for in-slab earthquakes in Indo-Burmese subduction zone. Soil Dynam. Earthq. Eng. 30 (5), 368–377.
Gutenberg, B., Richter, C.F., 1944. Frequency of earthquakes in California. Bull. Seismol. Soc. Am. 34 (4), 185–188.
Hanks, T.C., Kanamori, H., 1979. A moment magnitude scale. J. Geophys. Res. Solid Earth 84 (B5), 2348–2350.
Indian Meteorological Department (http://www.imd.gov.in).
International Seismological Centre (http://www.isc.ac.uk).
Iyengar, R.N., et al., 2010. Development of Probabilistic Seismic Hazard Map of India. Technical report. National Disaster Management Authority (NDMA), Govt. of India, New Delhi.
Iyengar, R.N., Ghosh, S., 2004. Microzonation of earthquake hazard in greater Delhi area. Curr. Sci. 87 (9), 1193–1202.
Jibson, R.W., 2007. Regression models for estimating coseismic landslide displacement. Eng. Geol. 91 (2–4), 209–218.
Jibson, R.W., 2011. Methods for assessing the stability of slopes during earthquakes—a retrospective. Eng. Geol. 122 (1–2), 43–50.
Joyner, W.B., Boore, D. M, 1981. Peak horizontal acceleration and velocity from strong-motion records including records from the 1979 Imperial Valley, California, earthquake. Bull. Seismol. Soc. Am. 71 (6), 2011–2038. https://doi.org/10.1785/BSSA0710062011.
Kanth, S.R., Iyengar, R.N., 2006. Seismic hazard estimation for Mumbai city. Curr. Sci. 1486–1494.
Kavand, A., Alielahi, H., 2017. Site-specific probabilistic seismic hazard analysis for northern part of the Qeshm Island, Iran. Nat. Hazards 88 (2), 919–946.
Kayal, J.R., 2001. Microearthquake activity in some parts of the Himalaya and the tectonic model. Tectonophysics 339 (3–4), 331–351.
Keefer, D.K., 1984. Landslides caused by earthquakes. Geol. Soc. Am. Bull. 95 (4), 406–421.
Khan, Z., El-Emam, M., Irfan, M., Abdalla, J., 2013. Probabilistic seismic hazard analysis and spectral accelerations for United Arab Emirates. Nat. Hazards 67 (2), 569–589.
Khattri, K.M., Tyagi, A.K., 1983. Seismicity patterns in the Himalayan plate boundary and identification of the areas of high seismic potential. Tectonophysics 96 (3–4), 281–297.
Khattri, K.N., Rogers, A.M., Perkins, D.M., Algermissen, S.T., 1984. A seismic hazard map of India and adjacent areas. Tectonophysics 108 (1–2), 93–134.
Kijko, A., 2004. Estimation of the maximum earthquake magnitude, m max. Pure Appl. Geophys. 161 (8), 1655–1681.
Kijko, A., Smit, A., Sellevoll, M.A., 2016. Estimation of earthquake hazard parameters from incomplete data files. Part III. Incorporation of uncertainty of earthquake-occurrence model. Bull. Seismol. Soc. Am. 106 (3), 1210–1222.
Knopoff, L., 1964. The statistics of earthquakes in Southern California. Bull. Seismol. Soc. Am. 54 (6A), 1871–1873.
Knopoff, L., Gardner, J.K., 1972. Higher seismic activity during local night on the raw worldwide earthquake catalogue. Geophys. J. Int. 28 (3), 311–313.
Kolathayar, S., Sitharam, T.G., 2012. Characterization of regional seismic source zones in and around India. Seismol Res. Lett. 83 (1), 77–85.
Kolathayar, S., Sitharam, T.G., Vipin, K.S., 2012. Spatial variation of seismicity parameters across India and adjoining areas. Nat. Hazards 60 (3), 1365–1379.
Kramer, S.L., 1996. Geotechnical Earthquake Engineering. Pearson Education India.
Krinitzsky, E.L., 2002. How to obtain earthquake ground motions for engineering design. Eng. Geol. 65 (1), 1–16.
Krishna, J., 1959, February. Seismic zoning of India. In: Earthquake Engineering Seminar. Roorkee University, India, pp. 32–38.
Kumar, P., Yuan, X., Kumar, M.R., Kind, R., Li, X., Chadha, R.K., 2007. The rapid drift of the Indian tectonic plate. Nature 449 (7164), 894–897.
Malik, S., Sharma, M.L., Khandelwal, D.D., 2006, December. Estimation of spectral strong ground motion for North East India using PSHA. In: 13th Symposium on Earthquake Engineering. Roorkee, pp. 18–20.
Manglik, A., Kumar, G.P., Thiagarajan, S., 2013. Transverse tectonics in the Sikkim Himalaya: a magnetotelluric study. Tectonophysics 589, 142–150.
Martha, T.R., Govindharaj, K.B., Kumar, K.V., 2015. Damage and geological assessment of the 18 September 2011 Mw 6.9 earthquake in Sikkim, India using very high resolution satellite data. Geosci. Front. 6 (6), 793–805.
MATLAB, 2018. 9.7.0.1190202 (R2019b). The MathWorks Inc, Natick, Massachusetts.
McGuire, R.K., 1976. FORTRAN Computer Program for Seismic Risk Analysis (No. 76-67). US Geological Survey.
McGuire, R.K., 1977. Effects of uncertainty in seismicity on estimates of seismic hazard for the east coast of the United States. Bull. Seismol. Soc. Am. 67 (3), 827–848.
Mezcua, J., Rueda, J., Blanco, R.M.G., 2011. A new probabilistic seismic hazard study of Spain. Nat. Hazards 59 (2), 1087–1108.
Mohanty, W.K., Verma, A.K., 2013. Probabilistic seismic hazard analysis for Kakrapar atomic power station, Gujarat, India. Nat. Hazards 69 (1), 919–952.
Mohanty, W.K., Walling, M.Y., 2008. Seismic hazard in mega city Kolkata, India. Nat. Hazards 47 (1), 39–54.
Molchan, G.M., Dmitrieva, O.E., 1992. Aftershock identification: methods and new approaches. Geophys. J. Int. 109 (3), 501–516.
Nath, S.K., Thingbaijam, K.K.S., 2011. Peak ground motion predictions in India: an appraisal for rock sites. J. Seismol. 15 (2), 295–315.
Nath, S.K., Thingbaijam, K.K.S., 2012. Probabilistic seismic hazard assessment of India. Seismol Res. Lett. 83 (1), 135–149.
Nath, S.K., Mandal, S., Adhikari, M.D., Maiti, S.K., 2017. A unified earthquake catalogue for South Asia covering the period 1900–2014. Nat. Hazards 85 (3), 1787–1810.
Nath, S.K., Raj, A., Thingbaijam, K.K.S., Kumar, A., 2009. Ground motion synthesis and seismic scenario in Guwahati city—a stochastic approach. Seismol Res. Lett. 80 (2), 233–242.
NDMA, 2010. Development of Probabilistic Seismic Hazard Map of India. technical report of the Working Committee of Experts (WCE), National Disaster Management Authority (NDMA). Govt. of India, New Delhi.
Parvez, I.A., Ram, A., 1997. Probabilistic assessment of earthquake hazards in the north-east Indian peninsula and Hindukush regions. Pure Appl. Geophys. 149 (4), 731–746.
Parvez, I.A., Vaccari, F., Panza, G.F., 2003. A deterministic seismic hazard map of India and adjacent areas. Geophys. J. Int. 155 (2), 489–508.

Priestley, K., Jackson, J., McKenzie, D., 2008. Lithospheric structure and deep earthquakes beneath India, the Himalaya and southern Tibet. Geophys. J. Int. 172 (1), 345–362.
Quittmeyer, R.C., Jacob, K.H., 1979. Historical and modern seismicity of Pakistan, Afghanistan, northwestern India, and southeastern Iran. Bull. Seismol. Soc. Am. 69 (3), 773–823.
Reasenberg, P., 1985. Second-order moment of central California seismicity, 1969–1982. J. Geophys. Res. Solid Earth 90 (B7), 5479–5495.
Reiter, L., 1990, 3. Earthquake Hazard Analysis: Issues and Insights, 22. Columbia University Press, New York, p. 254.
Roback, K., Clark, M.K., West, A.J., Zekkos, D., Li, G., Gallen, S.F., Godt, J.W., 2018. The size, distribution, and mobility of landslides caused by the 2015 Mw7. 8 Gorkha earthquake, Nepal. Geomorphology 301, 121–138.
Saygili, G., Rathje, E.M., 2008. Empirical predictive models for earthquake-induced sliding displacements of slopes. J. Geotech. Geoenviron. Eng. 134 (6), 790–803.
Scherbaum, F., Delavaud, E., Riggelsen, C., 2009. Model selection in seismic hazard analysis: an information-theoretic perspective. Bull. Seismol. Soc. Am. 99 (6), 3234–3247.
Scordilis, E.M., 2006. Empirical global relations converting MS and mb to moment magnitude. J. Seismol. 10 (2), 225–236.
Sharma, M.L., Douglas, J., Bungum, H., Kotadia, J., 2009. Ground-motion prediction equations based on data from the Himalayan and Zagros regions. J. Earthq. Eng. 13 (8), 1191–1210.
Shukla, J., Choudhury, D., 2012. Seismic hazard and site-specific ground motion for typical ports of Gujarat. Nat. Hazards 60 (2), 541–565.
Sil, A., Sitharam, T.G., Kolathayar, S., 2013. Probabilistic seismic hazard analysis of Tripura and Mizoram states. Nat. Hazards 68 (2), 1089–1108.
Silva, V., Crowley, H., Pagani, M., Monelli, D., Pinho, R., 2014. Development of the OpenQuake engine, the Global Earthquake Model's open-source software for seismic risk assessment. Nat. Hazards 72 (3), 1409–1427.
Sinha-Roy, S., 1982. Himalayan Main central Thrust and its implications for Himalayan inverted metamorphism. Tectonophysics 84 (2–4), 197–224.
Stepp, J.C., 1972, October. Analysis of completeness of the earthquake sample in the Puget Sound area and its effect on statistical estimates of earthquake hazard. In: Proc. Of the 1st Int. Conf. on Microzonazion, Seattle, 2, pp. 897–910.
Stewart, J.P., Douglas, J., Javanbarg, M., Bozorgnia, Y., Abrahamson, N.A., Boore, D.M., et al., 2015. Selection of ground motion prediction equations for the global earthquake model. Earthq. Spectra 31 (1), 19–45.
Tandon, A.N., 1956. Zones of India liable to earthquake damage. Indian J. Meteorol. Geophys. 10, 137–146.
Thenhaus, P.C., 1986. Seismic source zones in probabilistic estimation of the earthquake ground motion hazard: a classification with key issues. In: Proc. Workshop on Probabilistic Earthquake Hazard Assessments, pp. 85–185.
United States Geological Survey (https://www.usgs.gov/).
Utsu, T., 1961. A statistical study on the occurrence of aftershocks. Geophys. Mag. 30, 521–605.
Van Stiphout, T., Zhuang, J., Marsan, D., 2012. Seismicity Declustering. Community Online Resource for Statistical Seismicity Analysis. https://doi.org/10.5078/corssa-52382934.
Waseem, M., Lateef, A., Ahmad, I., Khan, S., Ahmed, W., 2019. Seismic hazard assessment of Afghanistan. J. Seismol. 23 (2), 217–242.
Wiemer, S., 2001. A software package to analyze seismicity: ZMAP. Seismol Res. Lett. 72 (3), 373–382.
Wiemer, S., Wyss, M., 2000. Minimum magnitude of completeness in earthquake catalogs: examples from Alaska, the western United States, and Japan. Bull. Seismol. Soc. Am. 90 (4), 859–869.
Xu, C., Xu, X., Yao, X., Dai, F., 2014. Three (nearly) complete inventories of landslides triggered by the May 12, 2008 Wenchuan Mw 7.9 earthquake of China and their spatial distribution statistical analysis. Landslides 11 (3), 441–461.
Zhang, P., Yang, Z.X., Gupta, H.K., Bhatia, S.C., Shedlock, K.M., 1999. Global Seismic Hazard Assessment Program (GSHAP) in Continental Asia.
Zhao, J.X., Irikura, K., Zhang, J., Fukushima, Y., Somerville, P.G., Asano, A., Ogawa, H., 2006. An empirical site-classification method for strong-motion stations in Japan using H/V response spectral ratio. Bull. Seismol. Soc. Am. 96 (3), 914–925.
Zhuang, J., Ogata, Y., Vere-Jones, D., 2002. Stochastic declustering of space-time earthquake occurrences. J. Am. Stat. Assoc. 97 (458), 369–380.